JOURNAL OF GUIDANCE, CONTROL, AND DYNAMICS
Vol. 43, No. 7, July 2020

Full-Order Solution to the Attitude Reset Problem for Kalman Filtering of Attitudes

Rajan Gill*
Swiss Federal Institute of Technology, 8092 Zurich, Switzerland
Mark W. Mueller†
University of California, Berkeley, Berkeley, California 94720
and
Raffaello D'Andrea‡
Swiss Federal Institute of Technology, 8092 Zurich, Switzerland

https://doi.org/10.2514/1.G004134

Kalman filtering of states including attitudes poses a challenge due to the constraints of the rotation manifold. One of the standard approaches is to consider a deviation attitude, in the form of a reduced three-vector parametrization, to some nominal reference attitude that the Kalman filter tracks. After an update to the statistics of this deviation, a reset step is performed that adjusts the reference attitude. This reset step adjusts the statistics of the deviation, which has commonly been ignored in the literature. This paper presents an algorithm for the case when the deviation is represented as a rotation vector. The adjustment to the mean and covariance after the reset operation is presented, assessed using Monte Carlo sampling, and compared to other approaches used in the literature. The final result may be easily implemented and is computationally inexpensive. Connections and comparisons to the multiplicative extended Kalman filter, the unscented quaternion estimator, and Lie-group Kalman filters are made, with simulations performed on a rigid-body example.

I. Introduction

DETERMINING the attitude of a rigid body in real time is a problem that was investigated during the space race of the 1960s [1] and is still a topic of research today [2–6]. Because of its computational efficiency and robustness, the Kalman filter is an ideal choice for many applications and has been used in numerous attempts to solve the real-time attitude estimation problem. However, applying the Kalman filter for estimating attitudes is not a trivial problem, as shown in the literature. This is largely attributed to the lack of a vector space structure of the common singularity-free attitude representations such as the Euler symmetric parameters, henceforth referred to as the unit quaternion, or rotation matrices. As a result, one has to be careful in defining a probabilistic description on such a space, let alone applying Kalman filtering tools. Yet, many works [7–14] neglected this fact by directly applying the Kalman filter to, e.g., estimating the unit-quaternion parametrization of attitudes. Others have indeed pointed out that, in doing so, the practical ramifications are an ill-conditioned or even a singular covariance matrix [15]. Other works have circumvented this problem, at least in the measurement update, using ad hoc solutions, namely, the prefiltering of measurements [15–17], which are known to produce suboptimal estimates [17], or purposely adhering to singular and highly nonlinear representations (i.e., Euler angles) to avoid the aforementioned problems [18].

In Ref. [19], a norm-constrained Kalman filter was introduced, which has direct applications for estimating the unit-quaternion parametrization for attitudes. This was done for the measurement update by determining the minimum mean squared error yielding Kalman update gain subject to the norm constraint of the state via Lagrange multipliers. This yields an additive correction to the covariance update, and it results in additional theoretical and computational complexity [20].

Another approach is to consider a lower-dimensional parametrization of a perturbation attitude, to some deterministic reference attitude, that is to be tracked by the Kalman filter; this approach can be attributed to Ref. [21] from 1969. This idea sparked a plethora of research [2,3,22–56]: some of which extended this general idea to other Bayesian inferencing schemes, such as particle filtering. In the literature, this framework is often referred to as the multiplicative (extended) Kalman filter (MEKF), the indirect Kalman filter, the sequential Kalman filter, and the error state Kalman filter. After every update to this perturbation state (through either prediction via a process model and/or from a measurement update), a so-called reset step is performed where the post-reset reference attitude is adjusted so that the post-reset perturbation state is zero mean. This reset step ensures that the reference attitude represents the mean attitude of the rigid body (see Sec. II.B; it is not clear if this interpretation was understood previously in the literature); but, more important, it ensures that the perturbation attitude state stays "small" so as to stay far away from singularities because no singularity-free three-vector parametrization of rotations exists [23].

It has been noted that there is confusion regarding the adjustment to the statistics after the reset step [15,20]. However, Ref. [15] presented the correct adjustment when the deviation attitude is represented by two times the Gibbs–Rodrigues vector (a similar adjustment was presented in Ref. [34] but differs by a square-root factor). In Ref. [20], the lingering confusion was more formally addressed by formulating the reset problem, presenting a first-order approximation to the exact adjustment for rotation vectors. A similar first-order transformation can be found in Ref. [57].

No covariance adjustment (zero-order) and the first-order approximations can still work in practice, as shown in the literature, if the rigid body of interest does not rotate too quickly with respect to the sampling time, if measurements agree well with the predicted measurements, or through tuning of the problem data. However, there will still be a loss in accuracy. The estimate using the algorithm developed herein using a full-order reset may be expected to be of higher quality in comparison to the previous approaches (examples can be found in Sec. V).

Received 8 October 2018; revision received 7 January 2020; accepted for publication 4 February 2020; published online 8 May 2020.

*Ph.D. Candidate, Institute for Dynamic Systems and Control, ML K35, Sonneggstrasse 3.
†Assistant Professor, Department of Mechanical Engineering, 5136 Etcheverry Hall.
‡Professor, Institute for Dynamic Systems and Control, ML K32.4, Sonneggstrasse 3.

In Sec. II, some preliminaries are discussed regarding rotations and probabilities. In particular, a rotation vector parametrization will be used to model the deviation attitude. In Sec. III, a general estimation problem setup is discussed, giving context for the attitude reset problem. Specifics regarding rotation kinematics typically encountered in rigid bodies are also presented, and a corresponding formulation is proposed; this formulation has the nice property of being exact in discrete time. In Sec. IV, the full-order attitude reset is presented, with Monte Carlo and singular value comparisons to the zero- and first-order approaches. If the reader would just like the solution to implement on, e.g., the measurement update for the MEKF [23] or the unscented quaternion estimator (USQUE) [26], or to upgrade the attitude reset for the extended Kalman filter (EKF) or the unscented Kalman filter (UKF) based on Ref. [20], they can jump to this section. In Sec. V, an example rigid body is considered, and various EKFs and UKFs are proposed and compared to other approaches in the literature [e.g., MEKF, Lie-group (LG)–UKF [4], and USQUE] via simulation. In particular, a computationally efficient approach is presented for the proposed EKF in Remark 4.

II. Rotations

A. Parameterization and Kinematics

Henceforth, rotation matrices will be used to represent attitudes for the purposes of the subsequent derivations, but it is trivial to replace them with the unit-quaternion counterpart for practical implementations. The full-order attitude reset map that will be developed remains the same in either case, as long as the perturbation attitude is represented as a rotation vector.

The set of rotations is denoted by

$$\mathcal{SO}(3) = \{R \in \mathbb{R}^{3x3} | R^{\mathrm{T}} R = I_{3\times 3}, \det(R) = 1\}$$

Note that this set is not closed under matrix addition; nor is it commutative under the matrix product. However, it does form a group with compositions of rotations made by their matrix product [58].

Given a three-vector $a = (a_1, a_2, a_3) \in \mathbb{R}^3$, let its skew-symmetric matrix be

$$[a\times] \coloneqq \begin{bmatrix} 0 & -a_3 & a_2 \\ a_3 & 0 & -a_1 \\ -a_2 & a_1 & 0 \end{bmatrix} \in \mathfrak{so}(3) \tag{1}$$

such that the cross product of a and another three-vector b is $a \times b = [a\times]b$, and $\mathfrak{so}(3)$ is the set of skew-symmetric matrices contained in $\mathbb{R}^{3x3}$. Similarly, the map that brings a skew-symmetric matrix A to its constituent three-vector is denoted by $[A]^{\vee}$; that is, $[[a\times]]^{\vee} = a$.

The set of skew-symmetric matrices can parameterize any rotation [59]; by extension, so can the three-vectors (because skew-symmetric matrices and three-vectors are isomorphic). This is realized using the following map:

$$\exp : \mathfrak{so}(3) \to \mathcal{SO}(3) \tag{2}$$

$$[a\times] \mapsto \sum_{k\geq 0} \frac{1}{k!}[a\times]^k = \begin{cases} I_{3\times 3} + \dfrac{\sin(\|a\|)}{\|a\|}[a\times] + \dfrac{1-\cos(\|a\|)}{\|a\|^2}[a\times]^2: & \|a\| \neq 0 \\ I_{3\times 3}: & \text{else} \end{cases} \tag{3}$$

where $\|\cdot\|$ denotes the two-norm of its vector argument. The vector a in the preceding equation is viewed as a rotation vector. Let $\log(\cdot)$ denote the corresponding inverse mapping given by

$$\log : \mathcal{SO}(3) \to \{[a\times] \in \mathfrak{so}(3) | \|a\| < \pi\} \tag{4}$$

$$R \mapsto \sum_{k\geq 1} \frac{(-1)^{k+1}}{k}(R - I_{3\times 3})^k = \begin{cases} \dfrac{\theta(R)}{2\sin(\theta(R))}(R - R^{\mathrm{T}}): & \theta(R) \neq 0 \\ 0_{3x3}: & \text{else} \end{cases} \tag{5}$$

where $\theta(R) \coloneqq \cos^{-1}((\mathrm{Tr}(R) - 1)/2)$. Note that $\log(\exp([a\times])) = a$ only if $\|a\| < \pi$; otherwise, wrapping will occur. See, e.g., Refs. [58–61] for a more thorough treatment.

Consider the following representation for an attitude $R \in \mathcal{SO}(3)$, representing the forward frame rotation from some arbitrary frame to some body-fixed frame of an object:

$$R \coloneqq R^{\mathrm{ref}} \exp([\delta\times]) \tag{6}$$

where δ can be viewed as a perturbation rotation vector to some reference rotation R^{ref}. The dynamics of this rotation vector are given as follows, with dependence on time t omitted [60]:

$$\dot{\delta} = \omega + \frac{1}{2}[\delta\times]\omega + \frac{2 - \|\delta\|\cot(\|\delta\|/2)}{2\|\delta\|^2}[\delta\times]^2\omega \tag{7}$$

$$\coloneqq \Gamma(\delta)^{-1}\omega \tag{8}$$

which hits singularity when $\|\delta\| = 2\pi$, ω is the relative angular velocity of the object expressed in the body frame, and

$$\Gamma : \mathbb{R}^3 \to \mathbb{R}^{3\times 3} \tag{9}$$

$$\delta \mapsto \Gamma(\delta) = \begin{cases} I_{3\times 3} - \dfrac{1-\cos(\|\delta\|)}{\|\delta\|^2}[\delta\times] + \dfrac{\|\delta\| - \sin(\|\delta\|)}{\|\delta\|^3}[\delta\times]^2: & \|\delta\| \neq 0 \\ I_{3\times 3}: & \text{else} \end{cases} \tag{10}$$

Interestingly, the map $\Gamma(\cdot)$ will also be of use for a Jacobian matrix in an EKF as shown in Sec. III, as well as for the attitude reset step in Sec. IV. Furthermore, $\Gamma(\delta)$ for $\|\delta\| \neq 0$ can be rewritten (see Appendix A; this equivalent map seems to have been discovered recently in Ref. [62] using a very different derivation) to yield

$$\Gamma(\delta) = \frac{1}{\|\delta\|^2}(\delta\delta^{\mathrm{T}} + [\delta\times](\exp([\delta\times])^{\mathrm{T}} - I_{3\times 3})) \tag{11}$$

which will reduce computation as compared to Ref. (10) if $\exp([\delta\times])$ is already computed, as will be the case in Sec. V.B.

It is worth noting that, to first order,

$$\Gamma(\delta) \approx I_{3\times 3} - \frac{1}{2}[\delta\times] \tag{12}$$

$$\Gamma(\delta)^{-1} \approx I_{3\times 3} + \frac{1}{2}[\delta\times] \tag{13}$$

Similarly, the dynamics can be defined directly on the rotation manifold and is given by

$$\dot{R} = R[\omega\times] \tag{14}$$

B. Mean Attitude

Similar to the discussion in Ref. [15], if δ is a random three-vector parametrization in Eq. (6) with probability distribution function (PDF) $p_\delta(\cdot)$, and thereby R is a random variable with distribution $p_R(\cdot)$, then naively taking the expectation of Eq. (6),

$$\underset{(R)}{E}[R] = \underset{(\delta)}{E}[R^{\text{ref}} \exp([\delta\times])] = \int_{\mathbb{R}^3} R^{\text{ref}} \exp([x\times]) p_\delta(x)\, \mathrm{d}x \tag{15}$$

is to some extent meaningless because the result will not be a rotation. This comes from the fact that $\mathcal{SO}(3)$ is not a vector space.

Thus, given a probabilistic description of δ, which will be done by the Kalman filter in the subsequent section, it is important to be clear on what the mean attitude is defined to be. First consider the vector space case: the mean $\mu_z \in \mathbb{R}^n$ of a random variable z with PDF $p_z(\cdot)$ is defined to be the one that satisfies [63]

$$0_{n\times 1} = \underset{(z)}{E}[z - \mu_z] = \int_{\mathbb{R}^n} (\bar{z} - \mu_z) p_z(\bar{z})\, \mathrm{d}\bar{z} \tag{16}$$

Similarly, the mean attitude herein is defined as the $\mu_R \in \mathcal{SO}(3)$ that satisfies

$$0_{3\times 1} = \underset{(R)}{E}[[\log(\mu_R^{\mathsf{T}} R)]^\vee] = \int_{\mathbb{R}^3} [\log(\mu_R^{\mathsf{T}} R^{\text{ref}} \exp([x\times]))]^\vee p_\delta(x)\, \mathrm{d}x \tag{17}$$

where the law of the unconscious statistician [64] is used to get the right-hand side. If δ is zero mean and small in the sense that all its random variates have a norm less than π, then

$$\int_{\mathbb{R}^3} [\log((R^{\text{ref}})^{\mathsf{T}} R^{\text{ref}} \exp([x\times]))]^\vee p_\delta(x)\, \mathrm{d}x = \int_{\mathbb{R}^3} x p_\delta(x)\, \mathrm{d}x = 0_{3\times 1} \tag{18}$$

Thus, in this case, the mean attitude is R^{ref}. This in part motivates the attitude reset step, where the statistics of δ will be transferred in such a way that, after the reset, the mean attitude is represented by R^{ref} and the post-reset perturbation attitude is small in the sense of being zero mean. When, for example, δ is a Gaussian random three-vector parametrization, and thus infinitely many variates have a norm equal to or larger than π, then Eq. (18) is only an approximation, albeit a good one if the tails are small.

III. Problem Setup and Solution Approach

Consider the general discrete-time process

$$\xi[k+1],\ R[k+1] = \bar{f}_k(\xi[k], R[k], \eta^{\text{proc}}[k]) \tag{19}$$

where $\eta^{\text{proc}}[k]$ is a zero mean white noise process, and $\xi[k]$ and $R[k]$ make up the system state (including the attitude) at time step k (both of which are random variables). If the dynamics of the system are inherently continuous [e.g., the kinematics of R as given by Eq. (14)], then the preceding can be obtained by some suitable discretization method.

However, it will be natural to work with the local parametrization [Eq. (6)] of the rotation using the rotation vector $\delta[k]$:

$$R[k] \coloneqq R_k^{\text{ref}} \exp([\delta[k]\times]) \tag{20}$$

where R_k^{ref} is the deterministic reference attitude at time k (time indexing of random series will be done with square brackets, and deterministic ones will be done with subscripts). The reasons for doing so are as follows:

1) As described in Sec. II.B, with the rotation vector living in a vector space, it is convenient to describe the statistics of $R[k]$ using the statistics of $\delta[k]$, particularly for computationally efficient Bayesian tracking schemes like the EKF or UKF, which presume Euclidean states. This is not exclusive to rotation vectors though because, e.g., the Gibbs–Rodrigues vector can be used as described in Ref. [23]. The Gibbs–Rodrigues vector may also be better at encoding large uncertainties [15]. However, rotation vectors may be more intuitive to work with, having the nice property that $\|\delta\|$ is the angle of rotation.

2) The process model [Eq. (19)] will generally involve a numerical integration scheme of the continuous-time kinematics [Eq. (14)]. Thus, to ensure that the numerical integration scheme does not violate the constraint that $R[k] \in \mathcal{SO}(3)$, a projection must be performed [65], which adds complexity (although minor in the case of unit quaternions). This is no longer an issue when integrating Eq. (8), which can be done via the following using the rotation vector composition rule [60] to avoid the singularity in Eq. (8):

$$\delta[k+1] = [\log(\exp([\delta[k]\times]) \exp([\bar{\delta}(\Delta t)\times]))]^\vee \eqqcolon f_{\text{rv}}(\delta[k], \bar{\delta}(\Delta t)) \tag{21}$$

where $\bar{\delta}(\Delta t)$ is the solution to Eq. (8) evaluated at the discretization step size Δt with initial condition $\bar{\delta}(0) = 0$. If $\omega(t)$ is constant over the time interval Δt, perhaps due to a measurement from a digital gyroscope sensor, then

$$\delta[k+1] = f_{\text{rv}}(\delta[k], \omega(t_k)\Delta t) \tag{22}$$

i.e., the Euler-integration scheme is exact, and where t_k is the sampled time corresponding to the discrete-time step k (i.e., $\omega[k] \coloneqq \omega(t_k)$).

3) For a certain application, it may be more natural to describe the propagation equations using the rotation vector if it is not based on the kinematics [Eq. (14)] (see, e.g., Refs. [66,67], which can be extended to three dimensions).

Thus, by using Eq. (20), the model [Eq. (19)] is transformed to the following:

$$x[k+1] = f_k(x[k], \eta^{\text{proc}}[k]) \tag{23}$$

with $x[k] \coloneqq (\xi[k], \delta[k]) \in \mathbb{R}^n$ as the new system state, and R_k^{ref} is absorbed into the function $f_k(\cdot,\cdot)$.

Additionally, the following generic measurement model is assumed:

$$y[k] = h_k(x[k], \eta^{\text{meas}}[k]) \tag{24}$$

where, again, R_k^{ref} is absorbed into the function $h_k(\cdot,\cdot)$.

Now, any Bayesian inferencing scheme can be used to track the statistics of the state $x[k]$ using models (23) and (24), such as the extended Kalman filter or the unscented Kalman filter.[§]

Remark 1: If the evolution of the rotation vector is as per the exact kinematics map [Eq. (21)], then the following Jacobians will be needed for the EKF:

$$\left.\frac{\partial f_{\text{rv}}(\delta, \Delta)}{\partial \delta}\right|_{\delta=0} = \Gamma^{-1}(\Delta) \exp([\Delta\times])^{\mathsf{T}} \tag{25}$$

$$\left.\frac{\partial f_{\text{rv}}(\delta, \Delta)}{\partial \Delta}\right|_{\delta=0} = I_{3\times 3} \tag{26}$$

See Appendix B for the derivation. For nonzero δ, it would become difficult to construct an analytical expression for the Jacobians.

Next, the notion of an attitude reset is introduced. After the statistics of $\delta[k]$ are updated, via a prior using Eq. (23) and/or a posterior using Eq. (24), then introduce a new deterministic attitude $R_k^{\text{ref,post}}$ and random variable $\delta^{\text{post}}[k]$ such that

$$R[k] = R_k^{\text{ref}} \exp([\delta[k]\times]) \eqqcolon R_k^{\text{ref,post}} \exp([\delta^{\text{post}}[k]\times]) \tag{27}$$

with the requirement that $\delta^{\text{post}}[k]$ be zero mean. Henceforth, the post-reset variables $R_k^{\text{ref,post}}$ and $\delta^{\text{post}}[k]$ replace the pre-reset ones of R_k^{ref}

[§]A particle filter could also be used. Although, one could elect to work directly on $\mathcal{SO}(3)$ instead of using the local parameterization [Eq. (6)]. However, the benefit of working with this local parametrization and employing the attitude reset is having (an approximation to) the mean attitude via R^{ref}, which is available immediately using Eq. (30), and applying the transformation [Eq. (31)] to each particle. Furthermore, the approach herein could be used in a hybrid Kalman–particle filter scheme; see, e.g., Refs. [68–72].

and $\delta[k]$, and the Bayesian tracking scheme continues on. The reasons for performing such an attitude reset are as follows:

1) If the propagation for $\delta[k]$ is performed using the exact propagation [Eq. (21)], then as mentioned in Remark 1, the Jacobians necessary for the covariance propagation in the EKF are hard to evaluate for nonzero mean $\delta[k]$.

2) Again, if the propagation is according to Eq. (21), the dynamics become exceedingly nonlinear for larger $\delta[k]$ (see Appendix B). Thus, it is in the best interest for algorithms such as the EKF or UKF to minimize the nonlinearity such that the statistics can be tracked as accurately as possible [68,73].

3) If the propagation is performed according to a numerical integration of the continuous-time kinematics [Eq. (7)], then the reset step must be performed to avoid $\delta[k]$ and its variates becoming large enough to hit singularity.

4) If $\delta[k]$ is zero mean, then as per Sec. II.B, the mean attitude is available immediately via R_k^{ref} rather than having to solve for it using the mean attitude definition [Eq. (17)].

In any case, the filter designer may choose to perform the attitude reset whenever they want. However, for the first two aforementioned points where the kinematics is used for prediction, the authors recommend performing the attitude reset after every prediction and measurement update step, as will be done in the example of Sec. V.

As in Ref. [20], the problem of how to perform Eq. (27) can be summarized succinctly as Problem 1 in the subsequent section. Note that the resulting transformation will also affect the cross statistics of $\delta[k]$ and $\xi[k]$.

IV. Attitude Reset Problem and Solution

Problem 1: Let δ be a random three-vector parametrization for which the PDF is known and $R^{\text{ref}} \in \mathcal{SO}(3)$ is some deterministic attitude. Determine a deterministic $R^{\text{ref,post}} \in \mathcal{SO}(3)$ and random variable $\delta^{\text{post}} \in \mathbb{R}^3$ such that the following are true:

$$R^{\text{ref}} \exp([\delta\times]) = R^{\text{ref,post}} \exp([\delta^{\text{post}}\times]) \tag{28}$$

$$\underset{(\delta^{\text{post}})}{E}[\delta^{\text{post}}] = 0_{3\times 1} \tag{29}$$

We present a solution to Problem 1 to the first order in δ^{post}: that is, assuming δ^{post} is small, but to full order in the pre-reset δ. This is a reasonable assumption because part of the problem requirements is for the mean of δ^{post} to be zero, which is some notion of small. Note that the related works of Ref. [20] and (indirectly) Ref. [57] present an approximate solution to Problem 1 with the additional assumption that the pre-reset vector δ is small.

Theorem 1: To first order in δ^{post}, the solution to Problem 1 is

$$R^{\text{ref,post}} = R^{\text{ref}} \exp([\mu\times]) \tag{30}$$

$$\delta^{\text{post}} = \Gamma(\mu)(\delta - \mu) \tag{31}$$

where $\mu \coloneqq \underset{(\delta)}{E}[\delta]$.

Proof: See Appendix C. A similar result, when δ represents two times the vector part of the unit quaternion, can be found in Appendix D. □

Remark 2: If the state $x[k]$ as mentioned in Sec. III is being tracked by an EKF or UKF, then the post-reset covariance is given by

$$\operatorname{diag}(I_{(n-3)\times(n-3)}, \Gamma(\mu)) \underset{(x[k])}{\operatorname{Var}}[x[k]] \operatorname{diag}(I_{(n-3)\times(n-3)}, \Gamma(\mu)^{\mathsf{T}}) \tag{32}$$

where $\operatorname{diag}(\cdot)$ forms a block-diagonal matrix from its arguments.

It is important to mention that Eq. (30) was only known to be true to first order in the pre-reset δ (and δ^{post}). As it turns out, this is also true to full order in the pre-reset δ. The previous works that have neglected adjusting the post-reset covariance can be viewed as taking $\Gamma(\mu)$ to zero order; that is,

$$\Gamma_0(\mu) \coloneqq I_{3\times 3} \approx \Gamma(\mu) \tag{33}$$

Similarly, the works [20,57] that, respectively, presented the first-order solutions

$$\Gamma_1(\mu) \coloneqq I_{3\times 3} - [\mu\times]/2 \approx \Gamma(\mu) \tag{34}$$

$$\Gamma_{\exp}(\mu) \coloneqq \exp(-[\mu\times]/2) \approx \Gamma(\mu) \tag{35}$$

are equivalent in the sense that they equal $\Gamma(\mu)$ to, at most, first order.

A. Monte Carlo Assessment

The accuracy of the proposed reset [Eqs. (30) and (31)] can be quantified via Monte Carlo sampling. Henceforth, the prescript ${}_{\text{MC}}(\cdot)$ will be used to denote the Monte Carlo specific variables. The pre-reset ${}_{\text{MC}}\delta$ are sampled from some to-be-defined probability distribution parameterized by some $l, c \in \mathbb{R}^3$. The post-reset ${}_{\text{MC}}\delta^{\text{post}}$ can be computed as suggested by Eqs. (30) and (28):

$${}_{\text{MC}}\delta^{\text{post}} \coloneqq [\log(\exp([-{}_{\text{MC}}\mu(l,c)\times]) \exp([{}_{\text{MC}}\delta\times]))]^{\vee} \tag{36}$$

where

$${}_{\text{MC}}\mu(l,c) \coloneqq \underset{({}_{\text{MC}}\delta|l,c)}{E}[{}_{\text{MC}}\delta] \tag{37}$$

Due to the use of the $\log(\cdot)$ operator, it is implied that all variates of ${}_{\text{MC}}\delta^{\text{post}}$ have norms less than π. The post-reset sample mean and variance are computed using Eq. (36) to see how well they conform to Eqs. (29) and (32) (with $n = 3$). This process is repeated for various probability distributions of ${}_{\text{MC}}\delta$ by randomly generating the parameters l and c, from which we can construct a distribution of errors in the post-reset mean and variance.

1. Error Metrics

Given $l, c \in \mathbb{R}^3$, the PDF for each component $i \in \{0, 1, 2\}$ of ${}_{\text{MC}}\delta$ is given by

$$p_{{}_{\text{MC}}\delta_i|l_i,c_i}(x) \coloneqq U(x, c_i - l_i/2, c_i + l_i/2) \tag{38}$$

where

$$U(x, a, b) \coloneqq \begin{cases} 1/(b-a): & x \in [a, b] \\ 0: & \text{else} \end{cases} \tag{39}$$

represents a uniform distribution. Using uniform distributions was intentional to avoid the wrapping caused by $\log(\cdot)$, assuming $\|l\|$ is sufficiently small. Note that ${}_{\text{MC}}\mu(l, c) = c$.

Given the parameters l and c, $2^{20} \approx 10^6$ particles are sampled and passed through the map given by Eq. (36), from which the post-reset sample mean ${}_{\text{MC}}\delta^{\text{post}}_{s.\text{mean}}(l, c)$ and sample covariance ${}_{\text{MC}}\delta^{\text{post}}_{s,\text{cov}}(l, c)$ are computed to yield the following absolute error metrics:

$$\epsilon_{\text{mean}}(l, c) \coloneqq \|{}_{\text{MC}}\delta^{\text{post}}_{s.\text{mean}}(l, c)\| \tag{40}$$

$$\epsilon_{\text{cov}}(l,c) \coloneqq \left\| {}_{\text{MC}}\delta^{\text{post}}_{s.\text{cov}}(l,c) - \Gamma({}_{\text{MC}}\mu(l,c)) \underset{({}_{\text{MC}}\delta|l,c)}{\operatorname{Var}}[{}_{\text{MC}}\delta] \Gamma({}_{\text{MC}}\mu(l,c))^{\mathsf{T}} \right\|_F \tag{41}$$

where $\|\cdot\|_F$ denotes the Frobenius norm of its matrix argument.

2. Ensemble Monte Carlo

We now draw various l and c to create an ensemble sample of mean errors $\epsilon_{\text{mean}}(l, c)$ and covariance errors $\epsilon_{\text{cov}}(l, c)$ as follows:

$$p_{l_i}(x) \coloneqq U(x, 0, 1), \qquad i = 0, 1, 2 \tag{42}$$

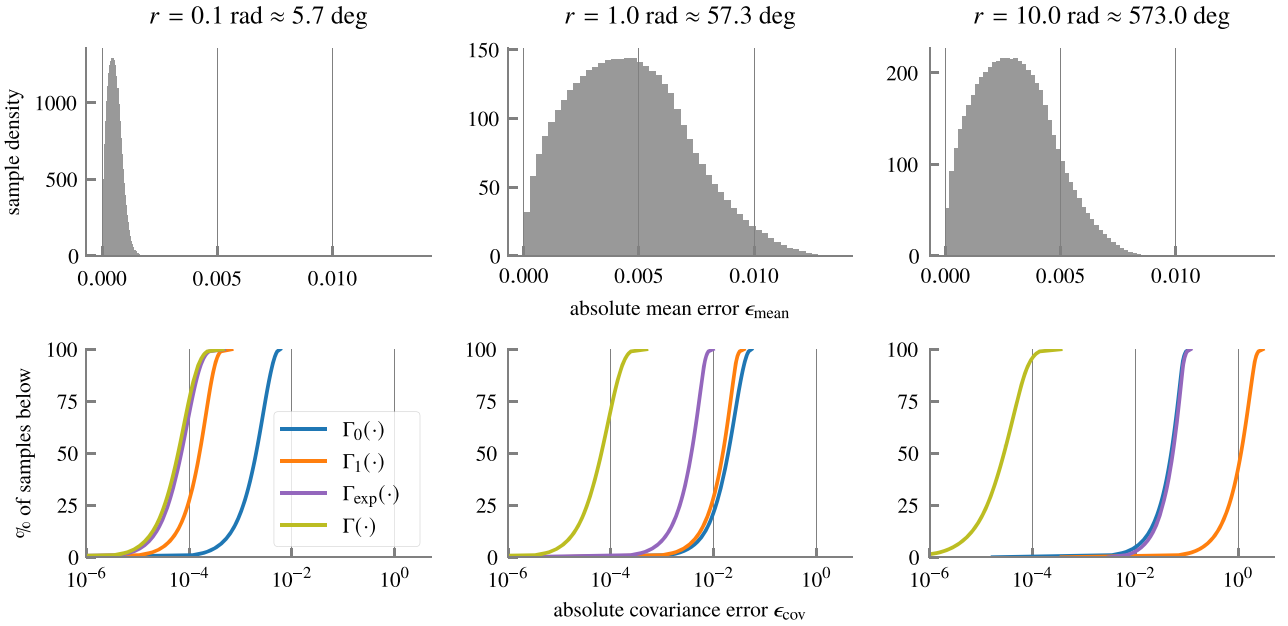

Fig. 1 Monte Carlo assessment: each column represents distinct r values, i.e., norm of mean pre-reset rotation vector: absolute mean errors as per Eq. (40) (top row); and absolute covariance errors as per Eq. (41) (bottom row) using approximate and exact $\Gamma(\cdot)$ maps.

and

$$c := \begin{bmatrix} r\cos(\theta)\cos(\phi) \\ r\sin(\theta)\cos(\phi) \\ r\sin(\phi) \end{bmatrix} \tag{43}$$

$$p_\theta(x) := U(x, -\pi, \pi) \tag{44}$$

$$p_\phi(x) := \begin{cases} \cos(x)/2: & x \in [-\pi/2, \pi/2] \\ 0: & \text{else} \end{cases} \tag{45}$$

which effectively and uniformly samples the sphere with radius r using the parametrization [Eq. (43)].

For each fixed r, $2^{20} \approx 10^6$ samples of l and c are drawn and thus 2^{20} values of $\epsilon_{\text{mean}}(l, c)$ and $\epsilon_{\text{cov}}(l, c)$ are depicted in Fig. 1 for each r. The covariance errors are also compared against the zero-order and first-order versions of the reset map $\Gamma(\cdot)$. The post-reset mean errors are all very small, regardless of the size of the pre-reset mean r, as expected due to Eq. (30) being exact in the pre-reset variable. For example, 95% of the samples have mean errors less than 0.0011, 0.0092, and 0.0060 for $r = 0.1$, 1, and 10 rad, respectively.

For rotations, it is only meaningful to report angles modulo π; but, for example, the angle may be larger if integrating the kinematics [Eq. (8)] directly or if the evolution of the rotation vector is not based on kinematics.

The covariance errors for the full-order map are consistently small and are noticeably better than the zero- and first-order versions, especially at the larger pre-reset means. As an example, the 95th percentile errors can be found in Table 1.

For the small r of 0.1, the first-order maps and the full-order map have errors in the same order of magnitude, with the full-order approach outperforming $\Gamma_1(\cdot)$ by a factor of two. However, this is not the case for $r = 1$ and 10 because the full-order approach outperforms the other approaches by orders of magnitude.

Table 1 95th percentile of absolute covariance errors

	r, rad		
	0.1	1.0	10
$\Gamma_0(\cdot)$	0.0044	0.042	0.085
$\Gamma_1(\cdot)$	0.00034	0.028	2.1
$\Gamma_{\text{exp}}(\cdot)$	0.00019	0.0069	0.086
$\Gamma(\cdot)$	0.00017	0.00018	0.000092

B. Closed-Form Comparison

The map $\Gamma(\cdot)$ can be compared to the zero-order and first-order approaches by means of a singular value analysis. Let

$$E_0(\mu) := \Gamma(\mu) - \Gamma_0(\mu) \tag{46}$$

$$= -\frac{1-\cos(\|\mu\|)}{\|\mu\|^2}[\mu\times] + \frac{\|\mu\| - \sin(\|\mu\|)}{\|\mu\|^3}[\mu\times]^2 \tag{47}$$

$$E_1(\mu) := \Gamma(\mu) - \Gamma_1(\mu) \tag{48}$$

$$= \left(-\frac{1-\cos(\|\mu\|)}{\|\mu\|^2} + \frac{1}{2}\right)[\mu\times] + \frac{\|\mu\| - \sin(\|\mu\|)}{\|\mu\|^3}[\mu\times]^2 \tag{49}$$

$$E_{\text{exp}}(\mu) := \Gamma(\mu) - \Gamma_{\text{exp}}(\mu) \tag{50}$$

$$= \left(-\frac{1-\cos(\|\mu\|)}{\|\mu\|^2} + \frac{\sin(\|\mu\|/2)}{\|\mu\|}\right)[\mu\times] + \left(\frac{\|\mu\| - \sin(\|\mu\|)}{\|\mu\|^3} - \frac{1-\cos(\|\mu\|/2)}{\|\mu\|^2}\right)[\mu\times]^2 \tag{51}$$

be the error matrices when $\mu \neq 0$, representing the difference between the full-order reset matrix $\Gamma(\mu)$ and the respective approximations used in literature. A reasonable scalar metric is the spectral norm (or largest singular value) given by [74]

$$\epsilon_i(\mu) := \|E_i(\mu)\| := \max_{\|x\|=1} \|E_i(\mu)x\| = \sqrt{\lambda_{\max}(E_i(\mu)^\top E_i(\mu))}, \quad i \in \{0, 1, \text{exp}\} \tag{52}$$

where $\lambda_{\max}(\cdot)$ denotes the maximum eigenvalue of its matrix argument. Observing that both error matrices have the structure of $c_1[\mu\times] + c_2[\mu\times]^2$ for some scalars c_1 and c_2, the following fact will prove useful:

Fact 1: Let $\mu \in \mathbb{R}^3$. The eigenvalue–eigenvector pairs of a matrix of the form

Table 2 Eigenvalues and eigenvectors for (53)

Eigenvalue	Eigenvector
0	μ
$(c_1\|\|\mu\|\|)^2 + (c_2\|\|\mu\|^2)^2$	$\mu^\perp$

$$(c_1[\mu\times] + c_2[\mu\times]^2)^\top (c_1[\mu\times] + c_2[\mu\times]^2) \tag{53}$$

are given by Table 2, where $\mu^\perp$ is a vector that satisfies $\mu^T\mu^\perp = 0$.

Proof: This is verifiable by direct substitution. □

Thus, by Fact 1,

$$\epsilon_0(\mu) = \frac{1}{\|\mu\|}\sqrt{\|\mu\|^2 - 2\|\mu\|\sin(\|\mu\|) - 2\cos(\|\mu\|) + 2} \tag{54}$$

$$\epsilon_1(\mu) = \frac{1}{2\|\mu\|}\sqrt{\|\mu\|^4 + 4\|\mu\|^2\cos(\|\mu\|) - 8\|\mu\|\sin(\|\mu\|) - 8\cos(\|\mu\|) + 8} \tag{55}$$

$$\epsilon_{\exp}(\mu) = 1 - \frac{2\sin(\|\mu\|/2)}{\|\mu\|} \tag{56}$$

Note that these errors do not depend on the direction of the argument μ but rather only its magnitude. Figure 2 shows the plots of the preceding error terms. Interestingly, there are domains over which the zero-order map is more accurate than the first-order approaches, which is consistent with the results in Fig. 1. It is useful to note that, for small $\|\mu\|$,

$$\epsilon_0(\mu) \approx \|\mu\|/2 \tag{57}$$

$$\epsilon_1(\mu) \approx \|\mu\|^2/6 \tag{58}$$

$$\epsilon_{\exp}(\mu) \approx \|\mu\|^2/24 \tag{59}$$

Loosely speaking, for a Kalman filtering application where the pre-reset mean is not large (that is, in the prediction step, either the sampling time is sufficiently small or the motion itself is slow; and corrections due to the measurements are small in the measurement update), the first-order map $\Gamma_1(\cdot)$ will be a very good approximation. Furthermore, additional terms from the series given in Eq. (B26) can be used for a better approximation. However, when computational expense is of no issue, the full-order map $\Gamma(\cdot)$, which already is of little complexity [and the same complexity as $\Gamma_{\exp}(\cdot)$], should always be used for improved accuracy. For implementations of the EKF/UKF that already use the zero- or first-order maps [Eqs. (33–35)] in the attitude reset, a simple replacement with $\Gamma(\cdot)$ yields an upgrade to a full-order attitude reset.

Remark 3: Although the EKF approximates the mean and covariance propagations to first and third orders, respectively [73], a lower-order attitude reset (independently) adds an additional source of error. For example, a measurement update could still lead to a large jump in the estimated state, and thus a full-order covariance reset will be beneficial to help mitigate the overall statistical tracking error; see Sec. V for an example. This can also be seen in Table 1, where for a pre-reset mean of 1 rad, the 95th percentile covariance errors for $\Gamma_1(\cdot)$ are 156 times as large as the 95th percentile covariances errors for the full-order $\Gamma(\cdot)$.

V. Rigid-Body Example

A. System

Consider the following rigid-body system:

$$\dot{p}(t) = v(t) \tag{60a}$$

$$\dot{v}(t) = R(t)a(t) \tag{60b}$$

$$\dot{R}(t) = R(t)[\omega(t)\times] \tag{60c}$$

where $p(t) \in \mathbb{R}^3$ is the position, $v(t) \in \mathbb{R}^3$ is the velocity, $R(t) \in \mathcal{SO}(3)$, $a(t) \coloneqq (1|\cos(t)|, 10|\sin(t)|, 100|\cos(t)|)$ m/s^2 is the body-frame acceleration vector, and $\omega(t) \coloneqq (10|\sin(t)|, 1|\cos(t)|, 0.1|\sin(t)|)$ rad/s is the body-frame angular velocity. The system is simulated numerically using the "embedded Runge–Kutta Prince–Dormand" method [75]. The initial conditions are set to $p(0) \coloneqq (100, 100, 100)$ m, $v(0) \coloneqq (10, 10, 10)$ m/s, and $R(0) \coloneqq \exp([(0, 0, \pi/2)\times])$.

Each estimator will have a noise-free accelerometer sensor that reads $a(t)$ and a gyroscope sensor that reads $\omega(t)$ but is corrupted with zero-mean white noise with a variance of 0.01 rad^2/s^2 per axis. Both sensors are digital and are read at a rate of 1000 Hz. Additionally, a Global-Positioning-System-like sensor provides position readings at 10 Hz and is also corrupted with zero-mean white noise with a variance of 100 m^2 per axis. It can be shown that the system is (locally) observable. All noise is generated from Gaussian distributions. All estimators are initialized to believe that the initial position and velocities are zero, and the initial attitude is given by the identity matrix.

The source code for the simulation and all filters tested can be found in Supplemental Material S1.

B. Proposed EKF

The system [Eq. (60)] is discretized using a sample rate of $\Delta t = 0.001$ s. The discretized model uses a combination of a simple Euler integration and the exact rotation propagation [Eq. (22)]:

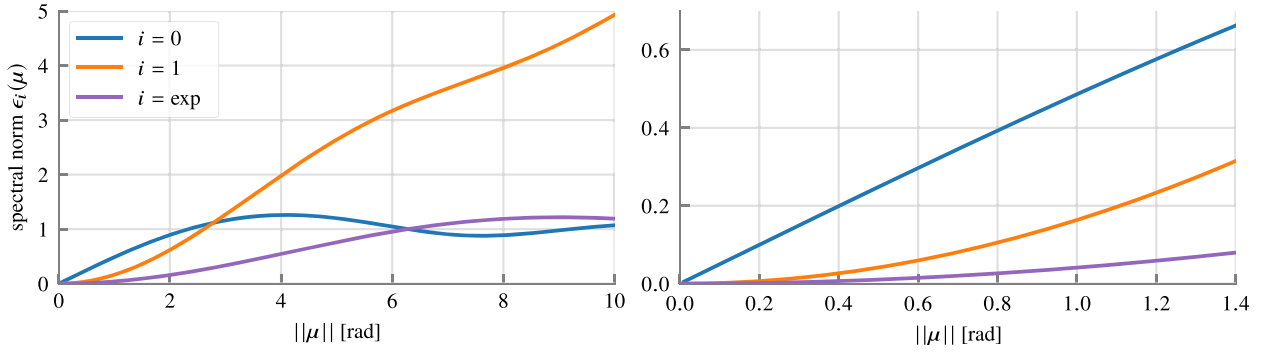

Fig. 2 Spectral norms of difference between full-order attitude reset matrix $\Gamma(\mu)$ and its zero-/first-order approximations, as defined in Eq. (52), over varying magnitudes of the rotation vector argument. Zoomed-in plot is shown on right.

$$\underbrace{\begin{bmatrix} p[k+1] \\ v[k+1] \\ \delta[k+1] \end{bmatrix}}_{=: x[k+1]} = \underbrace{\begin{bmatrix} p[k] + v[k]\Delta t + R_k^{\text{ref}} \exp([\delta[k]\times]) a_k \Delta t^2/2 \\ v[k] + R_k^{\text{ref}} \exp([\delta[k]\times]) a_k \Delta t \\ f_{\text{rv}}(\delta[k], (\omega[k] + \eta_\omega[k])\Delta t) \end{bmatrix}}_{=: f_k(x[k], \eta_\omega[k])} \tag{61}$$

with

$$\underset{(\eta_\omega[k])}{\text{Var}}[\eta_\omega[k]] = 0.01 I_{3\times 3}$$

and a_k is the deterministic body-frame acceleration measured at time step k. Now, applying the standard EKF formulas [73], we have, for the mean prediction step,

$$\hat{p}_{k+1|k} = \hat{p}_{k|k} + \hat{v}_{k|k}\Delta t + R_k^{\text{ref}} a_k \Delta t^2/2 \tag{62a}$$

$$\hat{v}_{k+1|k} = \hat{v}_{k|k} + R_k^{\text{ref}} a_k \Delta \tau \tag{62b}$$

$$\hat{\delta}_{k+1|k} = f_{\delta,\text{zoh}}(\hat{\delta}_{k|k}, \overline{\omega_k^{\text{meas}}}) = \overline{\omega_k^{\text{meas}}}\Delta t \tag{62c}$$

where $\overline{\omega_k^{\text{meas}}}$ is the realization of the random measurement (note that this gives the a priori mean if there is no prior knowledge available on the angular velocity); in Eq. (62c), it is assumed that $\hat{\delta}_{k|k} = 0$, i.e., an attitude reset was just performed beforehand. The covariance propagation is given by

$$\hat{P}_{k+1|k} = A_k \hat{P}_{k|k} A_k^\top + Q \tag{63a}$$

$$A_k = \left[\begin{array}{c|c|c} I_{3\times 3} & \Delta t I_{3\times 3} & -R_k^{\text{ref}}[a_k\times]\Delta t^2/2 \\ \hline 0_{3\times 3} & I_{3\times 3} & -R_k^{\text{ref}}[a_k\times]\Delta t \\ \hline 0_{3\times 3} & 0_{3\times 3} & \Gamma(\overline{\omega_k^{\text{meas}}}\Delta t)^{-1} \exp([-\overline{\omega_k^{\text{meas}}}\Delta t\times]) \end{array}\right] \tag{63b}$$

where $\hat{P}_{k+1|k}$ is the estimate of the a priori covariance of the state $x[k+1]$, with $\hat{P}_{0|0} := \text{diag}(I_{6\times 6}, 0.1 I_{3\times 3})$ for this and all following estimators; and $Q = \text{diag}(0_{6\times 6}, 0.01\Delta t^2 I_{3\times 3})$. Next, the attitude reset is applied as follows:

$$R_{k+1}^{\text{ref}} = R_k^{\text{ref}} \exp([\hat{\delta}_{k+1|k}\times]) \tag{64a}$$

$$\hat{P}_{k+1|k} \leftarrow \text{diag}(I_{6\times 6}, \Gamma(\hat{\delta}_{k+1|k})) \hat{P}_{k+1|k} \text{diag}(I_{6\times 6}, \Gamma(\hat{\delta}_{k+1|k})^\top) \tag{64b}$$

$$\hat{\delta}_{k+1|k} \leftarrow 0 \tag{64c}$$

Remark 4: The propagation equations [Eqs. (62–64)] can be combined, where the $\Gamma(\cdot)$ in Eq. (64b) cancels with the $\Gamma(\cdot)^{-1}$ in the Jacobian A_k, yielding the following consolidated propagation equations:

$$\hat{p}_{k+1|k} = \hat{p}_{k|k} + \hat{v}_{k|k}\Delta t + R_k^{\text{ref}} a_k \Delta t^2/2 \tag{65a}$$

$$\hat{v}_{k+1|k} = \hat{v}_{k|k} + R_k^{\text{ref}} a_k \Delta \tau \tag{65b}$$

$$\hat{\delta}_{k+1|k} = 0 \tag{65c}$$

$$R_{k+1}^{\text{ref}} = R_k^{\text{ref}} \exp([\overline{\omega_k^{\text{meas}}}\Delta t\times]) \tag{65d}$$

$$\hat{P}_{k+1|k} = \bar{A}_k \hat{P}_{k|k} \bar{A}_k^\top + \text{diag}(I_{6\times 6}, \Gamma(\overline{\omega_k^{\text{meas}}}\Delta t)) Q \text{diag}(I_{6\times 6}, \Gamma(\overline{\omega_k^{\text{meas}}}\Delta t)^\top) \tag{65e}$$

$$\bar{A}_k = \left[\begin{array}{c|c|c} I_{3\times 3} & \Delta t I_{3\times 3} & -R_k^{\text{ref}}[a_k\times]\Delta t^2/2 \\ \hline 0_{3\times 3} & I_{3\times 3} & -R_k^{\text{ref}}[a_k\times]\Delta t \\ \hline 0_{3\times 3} & 0_{3\times 3} & \exp([\overline{\omega_k^{\text{meas}}}\Delta t\times])^\top \end{array}\right] \tag{65f}$$

For computational efficiency, the $\exp([\overline{\omega_k^{\text{meas}}}\Delta t\times])^\top$ term in $\bar{A}_k$ should be computed first, and then $\Gamma(\overline{\omega_k^{\text{meas}}}\Delta t)$, for the transformation on Q, can be computed efficiently using the compact map [Eq. (11)].

The posterior, or measurement, update is given by

$$\begin{bmatrix} \hat{p}_{k|k} \\ \hat{v}_{k|k} \\ \hat{\delta}_{k|k} \end{bmatrix} = \begin{bmatrix} \hat{p}_{k|k-1} \\ \hat{v}_{k|k-1} \\ 0_{3\times 1} \end{bmatrix} + K_k(\overline{y_k^{\text{meas}}} - p_{k|k-1}) \tag{66a}$$

$$\hat{P}_{k|k} = (I_{9\times 9} - K_k C)\hat{P}_{k|k-1} \tag{66b}$$

where $C = [\, I_{3\times 3} \quad 0_{3\times 3} \quad 0_{3\times 3} \,]$, and K_k is the Kalman gain using the standard Kalman filter formulas [73]. Afterward, the attitude reset is applied again:

$$R_k^{\text{ref}} \leftarrow R_k^{\text{ref}} \exp([\hat{\delta}_{k|k}\times]) \tag{67a}$$

$$\hat{P}_{k|k} \leftarrow \text{diag}(I_{6\times 6}, \Gamma(\hat{\delta}_{k|k})) \hat{P}_{k|k} \text{diag}(I_{6\times 6}, \Gamma(\hat{\delta}_{k|k})^\top) \tag{67b}$$

$$\hat{\delta}_{k|k} \leftarrow 0 \tag{67c}$$

This algorithm is called "ekf-zoh-reset-F" in Fig. 3 because it is an EKF based on the exact propagation map [Eq. (22)] for a zero-order-hold assumption on the angular rates, and it uses a Full-order attitude reset.

Remark 5: It can be shown that the proposed EKF herein is equivalent to the LG-EKF of Ref. [76] when applied to the proposed model [Eq. (61)]. The difference is the derivation, where here it is done directly in the context of attitudes and using the attitude reset perspective. This may make it more accessible to formulate EKFs for other systems where, e.g., some inherent discrete-time process model is used directly for the rotation vector, as mentioned in Sec. III, allowing for a direct implementation without further derivations.

C. Other EKFs

One common EKF approach is to model the propagation of δ using an approximation for the rotation vector kinematics [Eq. (7)] [52,54–56,77]:

$$\delta[k+1] = \delta[k] + (I_{3\times 3} + [\delta[k]\times]/2)((\omega[k] + \eta_\omega[k])\Delta t) \tag{68}$$

and, when performing the attitude reset step in the prediction [Eq. (64)], to use a first-order approximation $\Gamma(\cdot) \approx \Gamma_1(\cdot)$. This results in the mean propagation being the same as Eq. (62). The covariance propagations are different, in that the $\Gamma(\overline{\omega_k^{\text{meas}}}\Delta t)^{-1} \exp([-\overline{\omega_k^{\text{meas}}}\Delta t\times])$ term in A_k in Eq. (63) is replaced with the approximation $I_{3\times 3} - [\overline{\omega_k^{\text{meas}}}\times]\Delta t/2$. The measurement updates are the same as Eq. (66), and the attitude reset step [Eq. (67)] after the measurement update is applied by again using the first-order approximation $\Gamma(\cdot) \approx \Gamma_1(\cdot)$. This algorithm is called "ekf-euler-reset-1" in Fig. 3 because the filter equations are equivalent to the case when an Euler discretization of the continuous-time kinematics of the rotation vector [Eq. (7)] is used; and a first-order approximation for the covariance resets is used (both during the prediction and measurement updates).

Another common variant is to take the ekf-euler-reset-1 filter and omit the postmeasurement covariance reset step [Eq. (67b)], and is called "ekf-euler-reset-0."

Figure 3 shows the estimator performances for the aforementioned EKFs. Both are able to recover the system state, but it is clear that the full-order "ekf-zoh-reset-F" is able to do this more quickly and much more consistently with less spread. What is interesting is that,

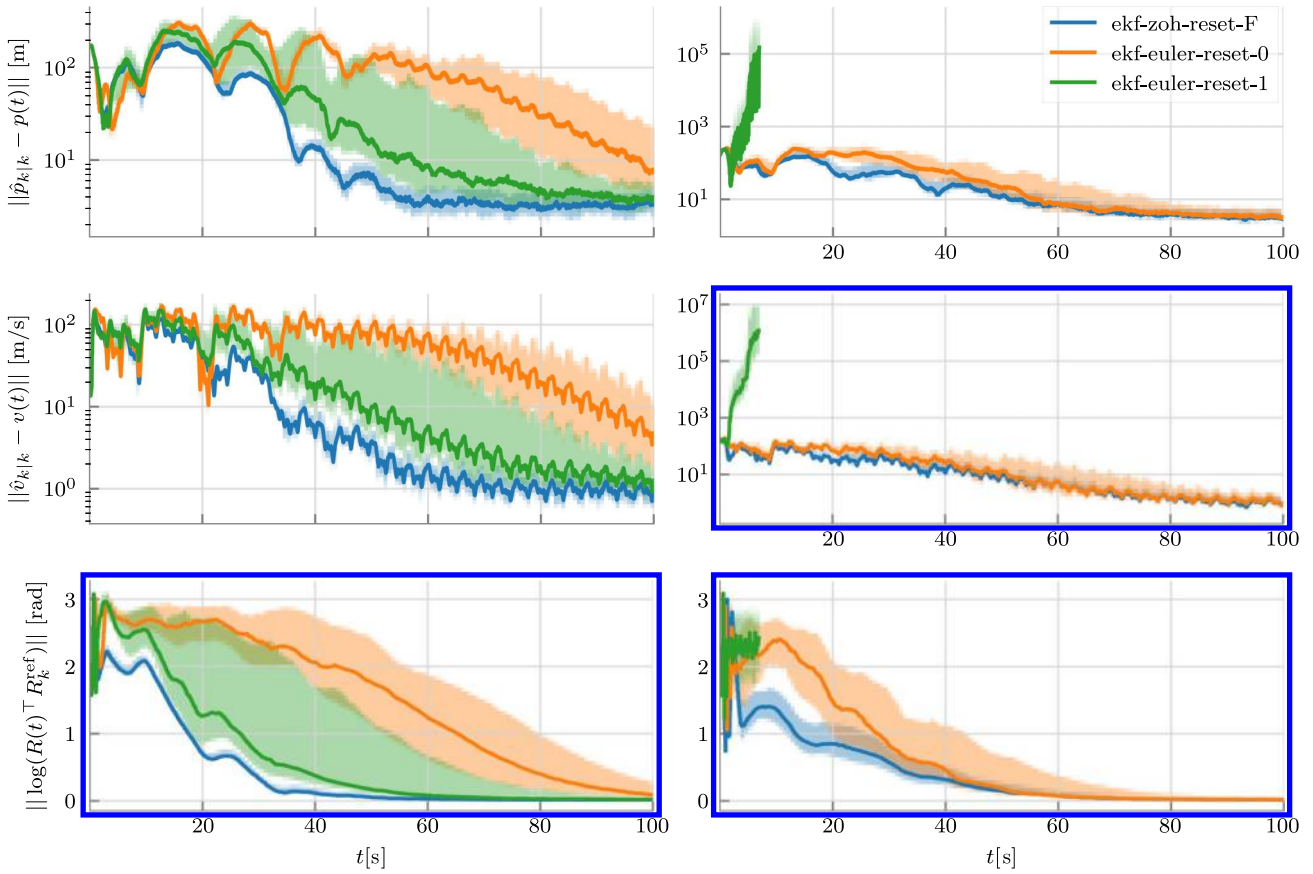

Fig. 3 Position, velocity, and attitude errors of EKFs described in Secs. V.B and V.C: 100 simulations performed, median values (solid lines), and 25th–75th percentile region (shaded regions). The right figure has an increased initial velocity error with $v(0) \coloneqq (100,100,100)$ m/s.

if the initial velocity error was to increase, such that $v(0) = (100, 100, 100)$ m/s, then the ekf-euler-reset-1 fails completely; see the right of Fig. 3. What happens here is that the covariance matrix becomes poorly conditioned, which can happen if δ becomes large in $\Gamma_1(\delta)$ when applying the covariance reset.

D. MEKF

1. Original

The MEKF algorithm of Ref. [23], which is formulated in continuous time, is adapted to fit the example rigid-body system [Eq. (60)]. The mean propagations are implemented in discrete time using Eqs. (65a–65d) for simplicity and consistency. The covariance propagation is adapted to fit the system, yielding

$$\dot{\hat{P}}(t) = F(t)\hat{P}(t) + \hat{P}(t)F(t)^\top + Q_c \tag{69a}$$

$$F(t) = \left[\begin{array}{c|c|c} 0_{3\times3} & I_{3\times3} & 0_{3\times3} \\ \hline 0_{3\times3} & 0_{3\times3} & -R_k^{\text{ref}} \exp([\overline{\omega_k^{\text{meas}}}(t-t_k)\times])[a_k\times] \\ \hline 0_{3\times3} & 0_{3\times3} & [-\overline{\omega_k^{\text{meas}}}\times] \end{array}\right] \tag{69b}$$

and $Q_c = \text{diag}(0_{6\times6}, 0.01\Delta t I_{3\times3})$ [73]. Because the covariance propagation is formulated in continuous time, they are implemented using an Euler-integration scheme, as was done in, e.g., Ref. [78] with a step size of Δt_{mekf} (see Algorithm 1) between successive discrete-time steps. Computational and implementation aspects favor using such a simple integration scheme, and more accurate integration will yield more accurate results; the parameter Δt_{mekf} will be varied to explore this. Note that no explicit attitude reset step is done in the prediction step because this is already done implicitly.

Algorithm 1: Euler integration of the MEKF covariance propagation [Eq. (69)]

input: Covariance matrix $\hat{P}_{k|k}$, sampled accelerometer and gyroscope measurements a_k and $\overline{\omega_k^{\text{meas}}}$, the reference attitude R_k^{ref}, integration step size Δt_{mekf}, and discretization time step Δt.
output: A priori covariance matrix $\hat{P}_{k+1|k}$.
$\hat{P}_{k+1|k} \leftarrow \hat{P}_{k|k}$
$N \leftarrow \Delta t / \Delta t_{\text{mekf}}$
for $j \leftarrow 1$ **to** N, **do**
  $F \leftarrow \left[\begin{array}{c|c|c} 0_{3\times3} & I_{3\times3} & 0_{3\times3} \\ \hline 0_{3\times3} & 0_{3\times3} & -R_k^{\text{ref}} \exp([\overline{\omega_k^{\text{meas}}}(j-1)\Delta t_{\text{mekf}}\times])[a_k\times] \\ \hline 0_{3\times3} & 0_{3\times3} & [-\overline{\omega_k^{\text{meas}}}\times] \end{array}\right]$
  $\hat{P}_{k+1|k} \leftarrow \hat{P}_{k+1|k} + (F\hat{P}_{k+1|k} + \hat{P}_{k+1|k}F^\top + Q_c)\Delta t_{\text{mekf}}$
end

The measurement update is the same as Eq. (66). The attitude reset following the update is also the same as Eq. (67), except that the covariance reset [Eq. (67b)] does not occur. This filter is called "mekf-0" in Fig. 4. In Fig. 4, the column is for $\Delta t_{\text{mekf}} = \Delta t = 0.001$ s and the right column is for $\Delta t_{\text{mekf}} = \Delta t/100 = 0.00001$ s, taking roughly 100 times the computation time. The ekf-zoh-reset-F from Sec. V.B is shown for reference.

2. Proposed Modifications

In the attitude reset following the measurement update, the step [Eq. (67b)] is performed. This filter is called "mekf-F". Another variant could be to use a first-order approximation $\Gamma(\cdot) \approx \Gamma_1(\cdot)$ in (67b), and is called "mekf-1."

As mentioned in Ref. [23], due to the approximations used to derive the filter, the deviation attitude δ in the MEKF can be inter-

preted to be either a rotation vector (as was done thus far), two times the Gibbs–Rodrigues vector, or two times the vector part of the unit quaternion. Thus, following the measurement update [Eq. (66)], two additional versions of the attitude reset [Eq. (67)] are tested: the first is with the $\exp(\cdot)$ map in Eq. (67a) replaced with $\exp^G(\cdot)$, mapping two times the Gibbs–Rodrigues vector to the rotation manifold (see, e.g., equation 18b in Ref. [23]); and $\Gamma(\cdot)$ in the covariance reset [Eq. (67b)] is replaced with $\Gamma^G(\cdot)$:

$$\Gamma^G(\delta) = \frac{1}{1 + \|\delta\|^2/4}(I_{3\times 3} - [\delta\times]/2) \tag{70}$$

the proof of which can be found in the appendix of Ref. [15]. This filter variant is called "mekf-G."

Similarly, the other variant is to replace the $\exp(\cdot)$ map in Eq. (67a) with $\exp^{\text{qv}}(\cdot)$, mapping two times the vector part of the unit quaternion to the rotation manifold (see, e.g., equation 18d from Ref. [23]); and $\Gamma(\cdot)$ in the covariance reset [Eq. (67b)] is replaced with $\Gamma^{\text{qv}}(\cdot)$:

$$\Gamma^{\text{qv}}(\delta) = \frac{1}{\sqrt{1 - \|\delta\|^2/4}}(I_{3\times 3} + [\delta\times]^2/4) - [\delta\times]/2 \tag{71}$$

the proof of which can be found in Appendix D. Note that $\Gamma^{\text{qv}}(\cdot)$ has a singularity and is ill-defined for $\|\delta\| \geq 4$, which can cause problems by creating an ill-conditioned covariance matrix for an application where large resets are to be applied. This filter variant is called "mekf-qv."

The results are shown in Fig. 4. The MEKF is sensitive to the integration scheme used to solve Eq. (69) because the figure on the left using the larger Δt_{mekf} causes all MEKF variants to perform worse than ekf-zoh-reset-F. Similar to the previous result in Fig. 3, the first-order "mekf-1" and the mekf-qv result in poorly conditioned covariance matrices, resulting in failure of the estimators, even though the mekf-0 is still able to recover the state trajectory (on average). The mekf-G also performs well, although with more spread than the ekf-zoh-reset-F.

The covariance propagation for the MEKF was derived by using the continuous-time kinematics and using the quaternion equivalent of Eq. (14). This is in contrast to the approach of the ekf-zoh-reset-F, where the covariance propagation is derived directly in discrete time using the exact discretization map [Eq. (22)]. Thus, it is expected that the MEKF performance (using the correct attitude resets) approaches the performance of the ekf-zoh-reset-F in the limit as $\Delta t_{\text{mekf}} \to 0$; although, for the MEKF, this means an increase in computational complexity [26]. This is exactly what happens for the smaller Δt_{mekf} on the right of Fig. 4, where now the full-order variants mekf-F, mekf-G, and mekf-qv perform similar to ekf-zoh-reset-F, in terms of both average performance and consistency, while outperforming the mekf-0 and mekf-1 variants.

E. Proposed UKF

Begin by generating the sigma points $x^{(i)}_{k|k} = \left(p^{(i)}_{k|k}, v^{(i)}_{k|k}, \delta^{(i)}_{k|k}\right)$, $i = 0, \ldots, 2n$ (with $n = 9$ in this case), for system (61) using the state covariance $\hat{P}_{k|k}$ and any sigma-point generation method [73,79]. Because the process noise is nonadditive in the dynamics map [Eq. (61)], the system state can be augmented to include the process noise, yielding six additional sigma points in this case. However, for simplicity and consistency with the other UKFs that will be discussed later, the process noise will be incorporated using the standard EKF approach. The sigma points are propagated forward:

$$x^{(i)}_{k+1|k} := f_k\left(x^{(i)}_{k|k}, 0\right), \qquad i = 0, \ldots, 2n \tag{72}$$

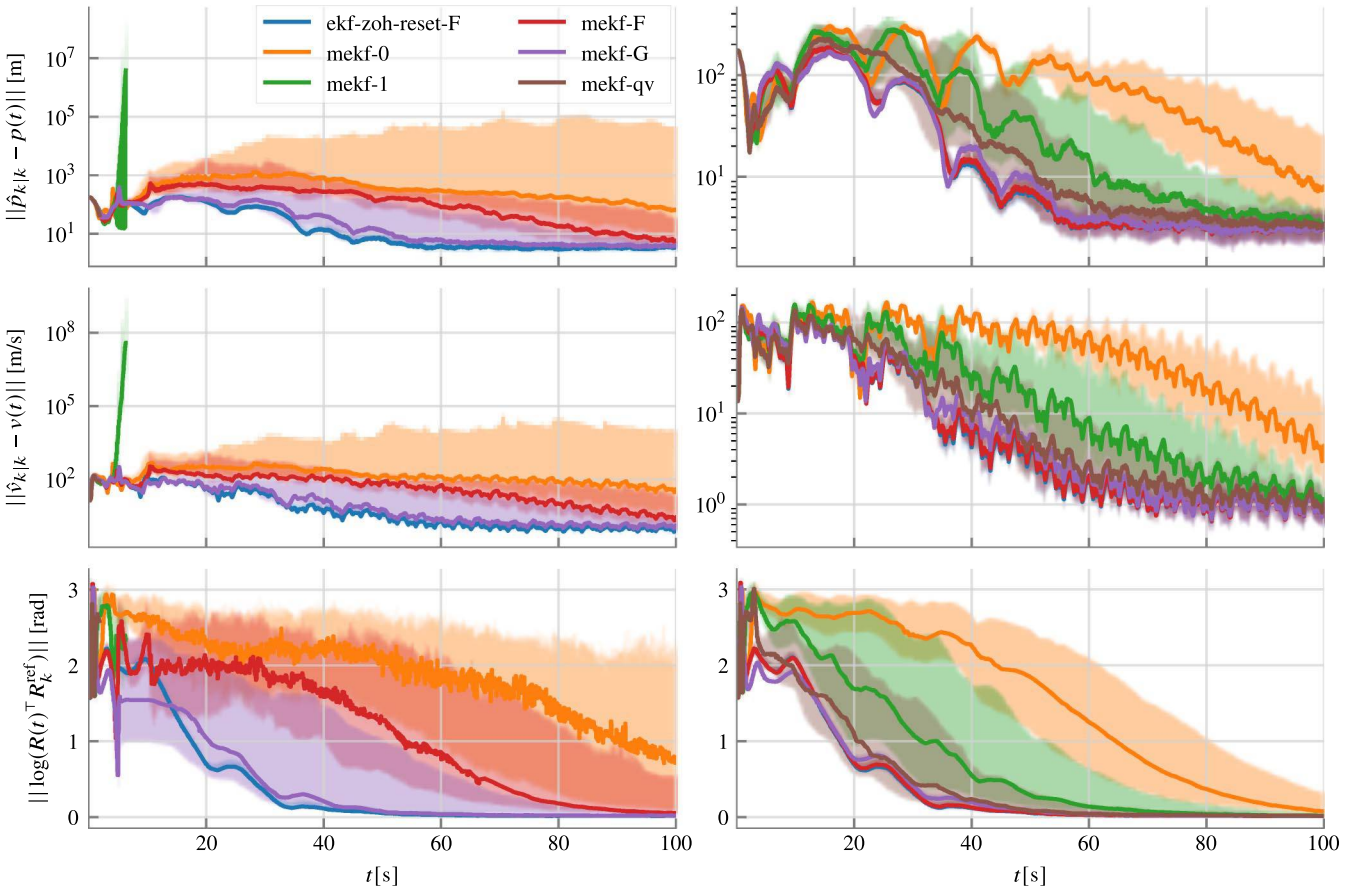

Fig. 4 Position, velocity, and attitude errors of MEKF using various attitude resets as described in Sec. V.D: 100 simulations performed, median values (solid lines), and 25th–75th percentile region (shaded regions). The left figure is for $\Delta t_{\text{mekf}} = \Delta t = 0.001$ s; the right figure is for $\Delta t_{\text{mekf}} = \Delta t/100 = 0.00001$ s, taking roughly 100 times the computation time. The ekf-zoh-reset-F from Sec. V.B is shown for reference.

The mean a priori state is then taken to be the weighted sum

$$\hat{x}_{k+1|k} \coloneqq \sum_{i=0}^{2n} w_m^{(i)} x_{k+1|k}^{(i)} \tag{73}$$

where $w_m^{(i)}$ are weighting coefficients [73,79]. Similarly, the a priori covariance is estimated

$$\hat{P}_{k+1|k} \coloneqq \sum_{i=0}^{2n} w_c^{(i)} (x_{k+1|k}^{(i)} - \hat{x}_{k+1|k})(x_{k+1|k}^{(i)} - \hat{x}_{k+1|k})^\top + Q \tag{74}$$

where $Q = \mathrm{diag}(0_{6\times6}, 0.01\Delta t^2 I_{3\times3})$ is the same as before, and $w_c^{(i)}$ are weighting coefficients [73,79]. Now, proceed with the postprediction attitude reset [Eq. (64)]. (The attitude reset presented herein is true to first order in the post-reset deviation attitude. Thus, for a situation where large uncertainty in the attitude is expected, the LG-UKF may perform better. Nevertheless, the proposed UKF can be viewed as an upgrade to the approach in Refs. [20,53].)

Because the measurement model is linear in the system state, the measurement update is the same as Eq. (66). The postmeasurement attitude reset [Eq. (67)] is applied. This filter is called "ukf-zoh-reset-F" in Fig. 5.

F. Lie Group–UKF

The LG-UKF algorithm of Ref. [4] is adapted to fit the example rigid-body system. The propagation equations are similar to the previous subsection, except that the sigma points for the rotation are computed directly on $\mathcal{SO}(3)$ as follows:

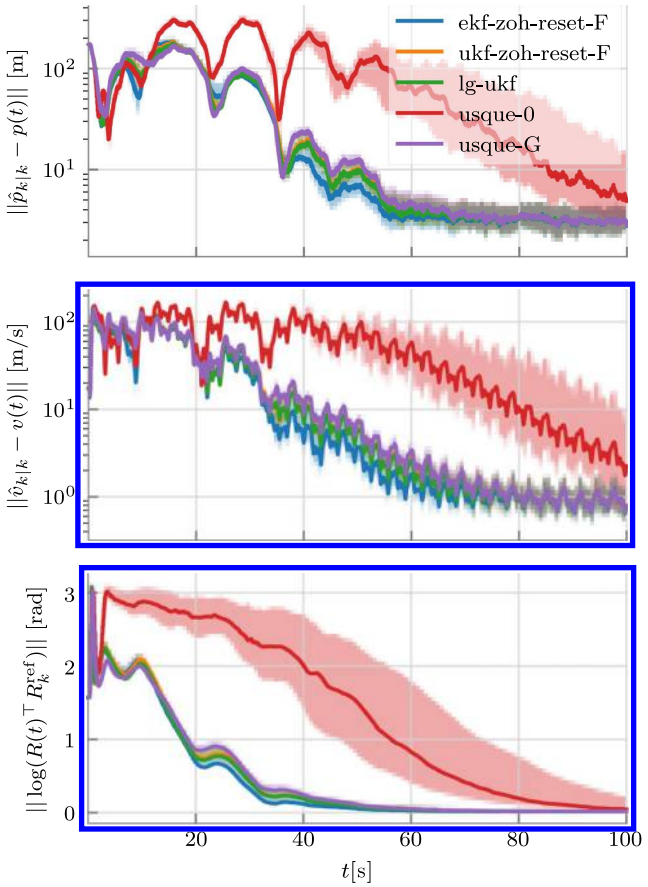

Fig. 5 Position, velocity, and attitude errors of UKFs described in Secs. V.E–V.G. 100 simulations performed, median values (solid lines), and 25th–75th percentile region (shaded regions). The ekf-zoh-reset-F from Sec. V.B is shown for reference.

$$R_{k+1|k}^{(i)} = R_k^{\mathrm{ref}} \exp([\delta_{k|k}^{(i)}\times]) \exp([\overline{\omega_k^{\mathrm{meas}}}\Delta t\times]), \quad i = 0,\ldots,2n \tag{75}$$

The mean rotation R_{k+1}^{ref} is computed numerically via Algorithm 1 of Ref. [4], which is written in Appendix E using the convention of this paper. The covariance propagation is computed as follows:

$$\hat{P}_{k+1|k} \coloneqq \sum_{i=0}^{2n} w_c^{(i)} d^{(i)} d^{(i)\top} + Q \tag{76}$$

$$d^{(i)} \coloneqq \left(p_{k+1|k}^{(i)} - \hat{p}_{k+1|k}, v_{k+1|k}^{(i)} - \hat{v}_{k+1|k}, \left[\log\left(\left(R_{k+1}^{\mathrm{ref}}\right)^{-1} R_{k+1|k}^{(i)}\right)\right]^\vee\right) \tag{77}$$

No attitude reset is performed because this is done implicitly. Furthermore, note that the process noise covariance matrix Q is not transformed because the approximation $\Gamma(\overline{\omega_k^{\mathrm{meas}}}\Delta t) \approx \Gamma_{\exp}(\overline{\omega_k^{\mathrm{meas}}}\Delta t)$ is used, which as shown in Sec. IV.B is a very good approximation for small $\overline{\omega_k^{\mathrm{meas}}}\Delta t$. This combined with the fact that Q is diagonal (as in Ref. [4] and in this case) results in

$$\mathrm{diag}(I_{6\times6}, \Gamma_{\exp}(\overline{\omega_k^{\mathrm{meas}}}\Delta t)) Q \mathrm{diag}(I_{6\times6}, \Gamma_{\exp}(\overline{\omega_k^{\mathrm{meas}}}\Delta t))^\top = Q$$

However, this will not be true for nonisotropic process noise.

The measurement update is the same as before in Eqs. (66–67). This filter is called "lg-ukf" in Fig. 5.

G. Unscented Quaternion Estimator

1. Original

The USQUE, presented in Ref. [26], is adapted to fit the example rigid-body system. As originally presented using the generalized Rodrigues parameters, two times the Gibbs–Rodrigues vector will be used herein. Thus, the $\exp(\cdot)$ map in system model (61), used to propagate the position and velocity sigma points, is replaced with the $\exp^G(\cdot)$ map. The rotation sigma points are propagated as follows:

$$R_{k+1|k}^{(i)} \coloneqq R_k^{\mathrm{ref}} \exp^G([\delta_{k|k}^{(i)}\times]) \exp([\overline{\omega_k^{\mathrm{meas}}}\Delta t\times]), \quad i = 0,\ldots,2n \tag{78}$$

However, based on Eqs. (36) and (37a) of Ref. [26], it is presumed that $R_{k+1|k}^{(0)}$ represents the mean a priori attitude, and thus $R_{k+1}^{\mathrm{ref}} \coloneqq R_{k+1|k}^{(0)}$. Because $\hat{\delta}_{k|k}^{(0)} = 0$, this essentially means that the USQUE does an EKF approximation for the mean attitude propagation [see, e.g., Eq. (65d)]. The covariance propagation is computed as follows:

$$\hat{P}_{k+1|k} \coloneqq \sum_{i=0}^{2n} w_c^{(i)} d^{(i)} d^{(i)\top} + Q \tag{79}$$

$$d^{(i)} \coloneqq \left(p_{k+1|k}^{(i)} - \hat{p}_{k+1|k}, v_{k+1|k}^{(i)} - \hat{v}_{k+1|k}, \left[\log^G\left(\left(R_{k+1}^{\mathrm{ref}}\right)^{-1} R_{k+1|k}^{(i)}\right)\right]^\vee\right) \tag{80}$$

where $\log^G(\cdot)$ maps the rotation element on $\mathcal{SO}(3)$ back to two times the Gibbs–Rodrigues vector (see, e.g., equation (20) of Ref. [26]). Thus, the USQUE is very similar to the LG-UKF, except that the mean attitude propagation is done using an EKF approximation, and the deviation attitude δ is viewed as two times the Gibbs–Rodrigues vector (or generalized Rodrigues parameters). Again, there is no transformation applied to the process noise covariance matrix Q (note that Ref. [26] did present a method for integrating Q_c using a trapezoidal integration scheme and under the assumption that $\omega\Delta t$ is small, which would result in adding a factor $Q/2$ to $\hat{P}_{k|k}$ when generating the sigma points in the propagation step, as well as replacing Q in Eq. (79) with the same factor, in this case). The measurement update is the same as before in Eq. (66) and the attitude reset [Eq. (67)] with $\exp(\cdot)$ replaced with $\exp^G(\cdot)$, except the covariance reset [Eq. (67b)] does not occur. This filter is called "usque-0" in Fig. 5.

2. Proposed Modification

One obvious modification is to perform the covariance adjustment after the measurement update [Eq. (67b)], with $\Gamma(\cdot)$ replaced with the Gibbs version $\Gamma^G(\cdot)$ given in Eq. (70); it will be called "usque-G." Another approach is to additionally perform a UKF mean propagation, which can be done by solving for the propagated mean either numerically, using an approach like the LG-UKF, or using an attitude reset approach like the proposed UKF. This, however, will not be explored in this paper.

The results for the aforementioned UKFs are shown in Fig. 5. The sigma points are generated using the scheme outlined in Sec. 14.2 of Ref. [73] and applying the scaling from Ref. [79] with $\alpha = 1$ and $\beta = 2$. The ekf-zoh-reset-F, ukf-zoh-reset-F, lg-ukf, and the usque-G all behave similarly, and they perform better than usque-0: both in terms of the average and consistency of errors.

VI. Conclusions

Theorem 1 establishes the relationship between the pre-reset and post-reset attitude error states to full order in the former and first order in the latter. This can be used in an EKF and UKF for a general problem setup involving attitudes. The proposed full-order reset step and the proposed EKF and UKF algorithms are computationally efficient and easy to implement. The full-order reset also offers a free upgrade to any of the zero- or first-order variants used in practice. Comparisons are also made with the MEKF and the USQUE using various attitude reset schemes, showing that a full-order reset can be beneficial.

Appendix A: Equivalent $\Gamma(\cdot)$ Map

By Ref. [74] (fact 3.5.25), $[a\times]^2 = aa^\top - \|a\|^2 I_{3\times3}$; thus, Eq. (10) can be rewritten to

$$\Gamma(a) = \frac{\sin(\|a\|)}{\|a\|} I_{3\times3} - \frac{1-\cos(\|a\|)}{\|a\|^2}[a\times] + \frac{\|a\| - \sin(\|a\|)}{\|a\|^3} aa^\top \tag{A1}$$

Rearranging,

$$\Gamma(a) = \frac{1}{\|a\|^2} aa^\top + \frac{\sin(\|a\|)}{\|a\|^3}(-aa^\top + \|a\|^2 I_{3\times3}) - \frac{1-\cos(\|a\|)}{\|a\|^2}[a\times] \tag{A2}$$

Again, by Ref. [74] (fact 3.5.25), $[a\times]^3 = -\|a\|^2[a\times]$; thus,

$$\Gamma(a) = \frac{1}{\|a\|^2} aa^\top + \frac{\sin(\|a\|)}{\|a\|^3}(-[a\times]^2) + \frac{1-\cos(\|a\|)}{\|a\|^4}[a\times]^3 \tag{A3}$$

$$= \frac{1}{\|a\|^2} aa^\top + \frac{1}{\|a\|^2}[a\times]\left(-\frac{\sin(\|a\|)}{\|a\|}[a\times] + \frac{1-\cos(\|a\|)}{\|a\|^2}[a\times]^2\right) \tag{A4}$$

$$= \frac{1}{\|a\|^2} aa^\top + \frac{1}{\|a\|^2}[a\times](\exp([-a\times]) - I_{3\times3}) \tag{A5}$$

$$= \frac{1}{\|a\|^2} aa^\top + \frac{1}{\|a\|^2}[a\times](\exp([a\times])^\top - I_{3\times3}) \tag{A6}$$

Appendix B: Derivation of the Jacobians for the Exact Kinematics Map

Lemma 1: If $X, Y, Z \in \mathfrak{so}(3)$ with

$$\exp(Z) = \exp(X)\exp(Y) \tag{B1}$$

then

$$Z = X + \frac{-\mathrm{ad}_X}{\exp(-\mathrm{ad}_X) - 1}(Y) + O(Y^2) \tag{B2}$$

$$= Y + \frac{\mathrm{ad}_Y}{\exp(\mathrm{ad}_Y) - 1}(X) + O(X^2) \tag{B3}$$

where ad denotes the matrix Lie-group adjoint mapping $\mathrm{ad}_X(Y) \coloneqq XY - YX$, the kth power of ad_X denotes its kth iterate with $\mathrm{ad}_X^0(Y) = Y$, and $\exp(A) = \sum_{k\geq0}(1/k!)A^k$. See Ref. [61] for a more thorough treatment.

Proof: Equation (B2) can be obtained by performing straightforward manipulations to the integral form of the Baker–Campbell–Hausdorff (BCH) formula (equation (5.8) of Ref. [61]).

For Eq. (B3), start with

$$\exp(Z(t)) = \exp(tX)\exp(Y) \tag{B4}$$

The goal is to determine $Z(1)$, with $Z(0) = Y$, minding the slight abuse of notation with Z versus $Z(t)$. Taking the derivative, from equation (5.11) of Ref. [61], we have

$$\frac{\mathrm{d}\exp(Z(t))}{\mathrm{d}t} = \exp(Z(t))\frac{1-\exp(-\mathrm{ad}_{Z(t)})}{\mathrm{ad}_{Z(t)}}(\dot{Z}(t))$$

$$= X\exp(tX)\exp(Y) \tag{B5}$$

$$= X\exp(Z(t)) \tag{B6}$$

Thus,

$$\frac{1-\exp(-\mathrm{ad}_{Z(t)})}{\mathrm{ad}_{Z(t)}}(\dot{Z}(t)) = \exp(-Z(t))X\exp(Z(t)) \tag{B7}$$

$$= \mathrm{Ad}_{\exp(-Z(t))}(X) \tag{B8}$$

$$= \exp(-\mathrm{ad}_{Z(t)})(X) \tag{B9}$$

where Ref. [61] (proposition 3.35) was used. Thus,

$$\dot{Z}(t) = \frac{\mathrm{ad}_{Z(t)}}{1-\exp(-\mathrm{ad}_{Z(t)})}\exp(-\mathrm{ad}_{Z(t)})(X) \tag{B10}$$

$$= \frac{\mathrm{ad}_{Z(t)}}{\exp(\mathrm{ad}_{Z(t)}) - 1}(X) \tag{B11}$$

$$= \frac{\log(\exp(\mathrm{ad}_{tX})\exp(\mathrm{ad}_Y))}{\exp(\mathrm{ad}_{tX})\exp(\mathrm{ad}_Y) - 1}(X) \tag{B12}$$

$$= \bar{g}(\exp(\mathrm{ad}_{tX})\exp(\mathrm{ad}_Y))(X) \tag{B13}$$

where Ref. [61] (theorem 3.28) was used,

$$\log(A) \coloneqq \sum_{k\geq1}\frac{(-1)^{k+1}}{k}(A-I)^k$$

and

$$\bar{g}(A) \coloneqq \sum_{k\geq0}\frac{(-1)^k}{k+1}(A-I)^k$$

Thus, an alternate integral form of the BCH is

$$Z = Y + \int_0^1 \bar{g}(\exp(\mathrm{ad}_{tX})\exp(\mathrm{ad}_Y))(X)\,\mathrm{d}t \tag{B14}$$

and thus, by performing straightforward manipulations, yields Eq. (B3). □

Using Eq. (B3), Eq. (21) becomes

$$f_{\mathrm{rv}}(\delta,\Delta)=\Delta+\Big[\underbrace{\frac{\mathrm{ad}_{[\Delta\times]}}{\exp(\mathrm{ad}_{[\Delta\times]})-1}([\delta\times])}_{=:[\xi\times]}+O([\delta\times]^2)\Big]^\vee \tag{B15}$$

where $\Delta \coloneqq \bar{\delta}(\Delta t)$ for brevity. Resolving the middle term,

$$\left(\frac{\exp(\mathrm{ad}_{[\Delta\times]})-1}{\mathrm{ad}_{[\Delta\times]}}\right)[\xi\times]=[\delta\times] \tag{B16}$$

$$\left(\exp(\mathrm{ad}_{[\Delta\times]})\frac{1-\exp(-\mathrm{ad}_{[\Delta\times]})}{\mathrm{ad}_{[\Delta\times]}}\right)[\xi\times]= \tag{B17}$$

Note that

$$[\mathrm{ad}_{[x\times]}([y\times])]^\vee=[([x\times][y\times]-[y\times][x\times])]^\vee \tag{B18}$$

$$=[x\times]y \tag{B19}$$

$$\Leftrightarrow [\mathrm{ad}^k_{[x\times]}([y\times])]^\vee=[x\times]^k y \tag{B20}$$

where the second equality comes from Ref. [74] (fact 3.5.25). Thus,

$$\left[(\exp(\mathrm{ad}_{[\Delta\times]})\frac{1-\exp(-\mathrm{ad}_{[\Delta\times]})}{\mathrm{ad}_{[\Delta\times]}})[\xi\times]\right]^\vee=\delta \tag{B21}$$

$$(\exp([\Delta\times])\frac{1-\exp(-[\Delta\times])}{[\Delta\times]})\xi= \tag{B22}$$

$$\exp([\Delta\times])\Gamma(\Delta)\xi= \tag{B23}$$

$$\Leftrightarrow \xi=\Gamma(\Delta)^{-1}\exp(-[\Delta\times])\delta \tag{B24}$$

where for the step from Eqs. (B22) to (B23), the following is used (a similar relationship can also be found in Refs. [80,81] without derivation):

$$\frac{1-\exp(-[\Delta\times])}{[\Delta\times]}=\frac{I-\sum_{k\geq 0}(-[\Delta\times])^k/k!}{[\Delta\times]} \tag{B25}$$

$$=\sum_{k\geq 0}\frac{(-1)^k}{(k+1)!}[\Delta\times]^k \tag{B26}$$

$$=\sum_{k\geq 0}\left(\frac{(-1)^{2k}}{(2k+1)!}[\Delta\times]^{2k}+\frac{(-1)^{2k+1}}{(2k+2)!}[\Delta\times]^{2k+1}\right) \tag{B27}$$

$$=\left(I_{3\times 3}+\sum_{k\geq 1}\frac{(-1)^{3k-1}\|\Delta\|^{2k-2}}{(2k+1)!}[\Delta\times]^2+\sum_{k\geq 0}\frac{(-1)^{3k+1}\|\Delta\|^{2k}}{(2k+2)!}[\Delta\times]\right) \tag{B28}$$

$$=\left(I_{3\times 3}+\sum_{k\geq 0}\frac{(-1)^{k}\|\Delta\|^{2k}}{(2k+3)!}[\Delta\times]^2+\sum_{k\geq 1}\frac{(-1)^{k}\|\Delta\|^{2k-2}}{(2k)!}[\Delta\times]\right) \tag{B29}$$

$$=\left(I_{3\times 3}+\frac{1}{\|\Delta\|^2}\left(1-\frac{1}{\|\Delta\|}\sum_{k\geq 0}\frac{(-1)^k\|\Delta\|^{2k+1}}{(2k+1)!}\right)[\Delta\times]^2+\frac{1}{\|\Delta\|^2}\left(\sum_{k\geq 0}\frac{(-1)^k\|\Delta\|^{2k}}{(2k)!}-1\right)[\Delta\times]\right) \tag{B30}$$

$$=\left(I_{3\times 3}+\frac{1}{\|\Delta\|^2}\left(1-\frac{1}{\|\Delta\|}\sin(\|\Delta\|)\right)[\Delta\times]^2+\frac{1}{\|\Delta\|^2}(\cos(\|\Delta\|)-1)[\Delta\times]\right) \tag{B31}$$

$$=\Gamma(\Delta) \tag{B32}$$

where the following is used to go from steps (B28) to (B29):

$$[x\times]^{2k+1}=(-1)^k\|x\|^{2k}[x\times],\qquad k=0,1,2,\ldots \tag{B33}$$

$$[x\times]^{2k}=(-1)^{k-1}\|x\|^{2k-2}[x\times]^2,\quad k=1,2,\ldots \tag{B34}$$

Thus,

$$f_{\mathrm{rv}}(\delta,\Delta)=\Delta+\Gamma(\Delta)^{-1}\exp([\Delta\times])^{\mathsf{T}}\delta+[O([\delta\times]^2)]^\vee \tag{B35}$$

from which Eqs. (25) and (26) are obtained. Note that, from Eq. (B35), the nonlinearity in the map increases as δ increases.

Appendix C: Solution to Problem 1

Because R^{ref}, $R^{\mathrm{ref,post}} \in \mathcal{SO}(3)$, there exists some deterministic $\mu \in \mathbb{R}^3$ such that

$$R^{\mathrm{ref}}\exp([\mu\times])=R^{\mathrm{ref,post}} \tag{C1}$$

Thus,

$$R^{\mathrm{ref}}\exp([\delta\times])=R^{\mathrm{ref,post}}\exp([\delta^{\mathrm{post}}\times]) \tag{C2}$$

$$\Rightarrow \exp([\delta\times])=\exp([\mu\times])\exp([\delta^{\mathrm{post}}\times]) \tag{C3}$$

Using Eq. (B2),

$$[\delta\times]=[\mu\times]+\frac{-\mathrm{ad}_{[\mu\times]}}{\exp(-\mathrm{ad}_{[\mu\times]})-1}([\delta^{\mathrm{post}}\times])+O([\delta^{\mathrm{post}}\times]^2) \tag{C4}$$

$$\Rightarrow \delta=\mu+\left[\frac{-\mathrm{ad}_{[\mu\times]}}{\exp(-\mathrm{ad}_{[\mu\times]})-1}([\delta^{\mathrm{post}}\times])+O([\delta^{\mathrm{post}}\times]^2)\right]^\vee \tag{C5}$$

Throwing away higher-order terms in δ^{post},

$$\delta\approx\mu+\frac{[\mu\times]}{I-\exp([-\mu\times])}\delta^{\mathrm{post}} \tag{C6}$$

Thus,

$$\delta^{\mathrm{post}}\approx\frac{I-\exp([-\mu\times])}{[\mu\times]}(\delta-\mu) \tag{C7}$$

$$=\Gamma(\mu)(\delta-\mu) \tag{C8}$$

where Eq. (B32) was used. The preceding is linear in the random variables δ and δ^{post}; therefore, constraint (29) implies that $\mu = \underset{(\delta)}{E}[\delta]$.

Appendix D: Solution to Problem 1 When δ Is Two Times the Vector Part of the Unit Quaternion

Rearranging Eq. (C3) and using quaternion algebra [82],

$$q(\delta^{\text{post}}) = q(-\mu) \odot q(\delta) \tag{D1}$$

where

$$q{:}\{x \in \mathbb{R}^3 | \|x\| \leq 2\} \to \{(a, v), a \in \mathbb{R}, v \in \mathbb{R}^3 | |a|^2 + \|v\|^2 = 1\} \tag{D2}$$

$$x \mapsto \begin{bmatrix} a \\ v \end{bmatrix} = \frac{1}{2} \begin{bmatrix} \sqrt{4 - \|x\|^2} \\ x \end{bmatrix} \tag{D3}$$

maps two times the vector part of the unit quaternion to the unit quaternion [23], and

$$q_1 \odot q_2 = (a_1, v_1) \odot (a_2, v_2) = \begin{bmatrix} a_1 a_2 - v_1^\top v_2 \\ a_1 v_2 + a_2 v_1 + v_1 \times v_2 \end{bmatrix} \tag{D4}$$

Thus,

$$a_\delta^{\text{post}} = a_\mu a_\delta + \mu^\top \delta / 4 \tag{D5}$$

$$\delta^{\text{post}} = a_\mu \delta - a_\delta \mu + \delta \times \mu / 2 \tag{D6}$$

where $a_\mu = \sqrt{1 - \|\mu\|^2/4}$ and $a_\delta = \sqrt{1 - \|\delta\|^2/4}$. Continuing,

$$\delta^{\text{post}} = \frac{a_\mu^2 \delta - a_\mu a_\delta \mu}{a_\mu} - \mu \times \delta / 2 \tag{D7}$$

$$= \frac{a_\mu^2 \delta - (a_\delta^{\text{post}} - \mu^\top \delta / 4)\mu}{a_\mu} - \mu \times \delta / 2 \tag{D8}$$

$$= \frac{a_\mu^2 \delta - (\sqrt{1 - \|\delta^{\text{post}}\|^2/4} - \mu^\top \delta / 4)\mu}{a_\mu} - \mu \times \delta / 2 \tag{D9}$$

$$= \frac{a_\mu^2 \delta - (1 + O(\|\delta^{\text{post}}\|^2) - \mu^\top \delta / 4)\mu}{a_\mu} - \mu \times \delta / 2 \tag{D10}$$

As in Appendix C, throwing away high-order terms in δ^{post},

$$\delta^{\text{post}} \approx \frac{a_\mu^2 \delta - (1 - \mu^\top \delta / 4)\mu}{a_\mu} - \mu \times \delta / 2 \tag{D11}$$

$$= \frac{(1 - \|\mu\|^2/4)\delta - (1 - \mu^\top \delta / 4)\mu}{\sqrt{1 - \|\mu\|^2/4}} - \mu \times \delta / 2 \tag{D12}$$

Using Ref. [74] (fact 3.5.25), $[\mu\times]^2 = \mu\mu^\top - \|\mu\|^2 I_{3\times 3}$; and noting that $[\mu\times]\mu = 0$, the preceding becomes

$$\delta^{\text{post}} \approx \Gamma^{\text{qv}}(\mu)(\delta - \mu) \tag{D13}$$

where $\Gamma^{\text{qv}}(\cdot)$ is given in Eq. (71). The preceding is linear in the random variables δ and δ^{post}; therefore, constraint (29) implies that $\mu = \underset{(\delta)}{E}[\delta]$. The authors would like to acknowledge one of the reviewers for this result.

Appendix E: Computation of the Mean Attitude for the LG-UKF

Algorithm 2: Weighted intrinsic mean on $\mathcal{SO}(3)$.

input: Set of rotations $R^{(i)}$ with associated weights $w_m^{(i)}$, $i = 0, \ldots, n$, and an integer $N > 0$.
output: The weighted mean R^{ref}.
$R^{\text{ref}} \leftarrow R^{(0)}$;
for $j \leftarrow 0$ **to** N, **do**
  $\Delta \leftarrow \sum_{i=0}^{n} w_m^{(i)} \log(R^{\text{ref}^{-1}} R^{(i)})$;
  $R^{\text{ref}} \leftarrow R^{\text{ref}} \exp(\Delta)$;
end

Acknowledgments

The authors would like to thank Landis Markley for his feedback and helpful comments to improve this paper. This research was funded by Swiss National Science Foundation grant number 200021_162365 and by the Natural Sciences and Engineering Research Council of Canada CGS-D scholarship.

References

[1] Grewal, M. S., and Andrews, A. P., "Applications of Kalman Filtering in Aerospace 1960 to the Present [Historical Perspectives]," *IEEE Control Systems Magazine*, Vol. 30, No. 3, 2010, pp. 69–78. https://doi.org/10.1109/MCS.2010.936465

[2] Stovner, B. N., Johansen, T. A., Fossen, T. I., and Schjølberg, I., "Attitude Estimation by Multiplicative Exogenous Kalman Filter," *Automatica*, Vol. 95, Sept. 2018, pp. 347–355. https://doi.org/10.1016/j.automatica.2018.05.038

[3] Eliahu, D. S., Elkaim, G. H., and Curry, R. E., "A Two-Stage Multiplicative Kalman Filter for Attitude Estimation of the Human Wrist," *IEEE/ION Position, Location and Navigation Symposium*, IEEE Publ., Piscataway, NJ, 2018, pp. 666–672. https://doi.org/10.1109/PLANS.2018.8373441

[4] Kang, D., Jang, C., and Park, F. C., "Unscented Kalman Filtering for Simultaneous Estimation of Attitude and Gyroscope Bias," *IEEE/ASME Transactions on Mechatronics*, Vol. 24, No. 1, 2019, pp. 350–360. https://doi.org/10.1109/TMECH.2019.2891776

[5] Chiella, A. C. B., Teixeira, B. O. S., and Pereira, G. A. S., "Quaternion-Based Robust Attitude Estimation Using an Adaptive Unscented Kalman Filter," *Sensors*, Vol. 19, No. 10, 2019, Paper 2372. https://doi.org/10.3390/s19102372

[6] Bernal-Polo, P., and Martínez-Barberá, H., "Kalman Filtering for Attitude Estimation with Quaternions and Concepts from Manifold Theory," *Sensors*, Vol. 19, No. 1, 2019, Paper 149. https://doi.org/10.3390/s19010149

[7] Yun, X., and Bachmann, E. R., "Design, Implementation, and Experimental Results of a Quaternion-Based Kalman Filter for Human Body Motion Tracking," *IEEE Transactions on Robotics*, Vol. 22, No. 6, 2006, pp. 1216–1227. https://doi.org/10.1109/TRO.2006.886270

[8] Sabatini, A. M., "Quaternion-Based Extended Kalman Filter for Determining Orientation by Inertial and Magnetic Sensing," *IEEE Transactions on Biomedical Engineering*, Vol. 53, No. 7, 2006, pp. 1346–1356. https://doi.org/10.1109/TBME.2006.875664

[9] Kingston, D., and Beard, R., "Real-Time Attitude and Position Estimation for Small UAVs Using Low-Cost Sensors," *AIAA 3rd "Unmanned Unlimited" Technical Conference, Workshop and Exhibit*, AIAA Paper 2004-6488, 2004. https://doi.org/10.2514/6.2004-6488

[10] de Marina, H. G., Pereda, F. J., Giron-Sierra, J. M., and Espinosa, F., "UAV Attitude Estimation Using Unscented Kalman Filter and TRIAD," *IEEE Transactions on Industrial Electronics*, Vol. 59, No. 11, 2012, pp. 4465–4474. https://doi.org/10.1109/TIE.2011.2163913

[11] Yun, X., Lizarraga, M., Bachmann, E. R., and McGhee, R. B., "An Improved Quaternion-Based Kalman Filter for Real-Time Tracking of Rigid Body Orientation," *IEEE/RSJ International Conference on Intelligent Robots and Systems*, Vol. 2, IEEE Publ., Piscataway, NJ, 2003, pp. 1074–1079. https://doi.org/10.1109/IROS.2003.1248787

[12] Bar-Itzhack, I., and Oshman, Y., "Attitude Determination from Vector Observations: Quaternion Estimation," *IEEE Transactions on Aero-*

space and Electronic Systems, Vol. AES-21, No. 1, 1985, pp. 128–136. https://doi.org/10.1109/TAES.1985.310546

[13] Marins, J. L., Yun, X., Bachmann, E. R., McGhee, R. B., and Zyda, M. J., "An Extended Kalman Filter for Quaternion-Based Orientation Estimation Using MARG Sensors," *IEEE/RSJ International Conference on Intelligent Robots and Systems*, Vol. 4, IEEE Publ., Piscataway, NJ, 2001, pp. 2003–2011. https://doi.org/10.1109/IROS.2001.976367

[14] Feng, K., Li, J., Zhang, X., Shen, C., Bi, Y., Zheng, T., and Liu, J., "A New Quaternion-Based Kalman Filter for Real-Time Attitude Estimation Using the Two-Step Geometrically-Intuitive Correction Algorithm," *Sensors*, Vol. 17, No. 9, 2017, p. 2146. https://doi.org/10.3390/s17092146

[15] Markley, F. L., "Lessons Learned," *Journal of the Astronautical Sciences*, Vol. 57, Jan. 2009, pp. 3–29, https://doi.org/10.1007/BF03321491

[16] Li, D., Landry, R., and Lavoie, P., "Low-Cost MEMS Sensor-Based Attitude Determination System by Integration of Magnetometers and GPS: A Real-Data Test and Performance Evaluation," *IEEE/ION Position, Location and Navigation Symposium*, IEEE Publ., Piscataway, NJ, 2008, pp. 1190–1198. https://doi.org/10.1109/PLANS.2008.4570005

[17] Crassidis, J. L., Markley, F. L., and Cheng, Y., "Survey of Nonlinear Attitude Estimation Methods," *Journal of Guidance, Control, and Dynamics*, Vol. 30, No. 1, 2007, pp. 12–28. https://doi.org/10.2514/1.22452

[18] Gross, J. N., Gu, Y., Rhudy, M. B., Gururajan, S., and Napolitano, M. R., "Flight-Test Evaluation of Sensor Fusion Algorithms for Attitude Estimation," *IEEE Transactions on Aerospace and Electronic Systems*, Vol. 48, No. 3, 2012, pp. 2128–2139. https://doi.org/10.1109/TAES.2012.6237583

[19] Zanetti, R., Majji, M., Bishop, R. H., and Mortari, D., "Norm-Constrained Kalman Filtering," *Journal of Guidance, Control, and Dynamics*, Vol. 32, No. 5, 2009, pp. 1458–1465. https://doi.org/10.2514/1.43119

[20] Mueller, M. W., Hehn, M., and D'Andrea, R., "Covariance Correction Step for Kalman Filtering with an Attitude," *Journal of Guidance, Control, and Dynamics*, Vol. 40, No. 9, 2016, pp. 2301–2306. https://doi.org/10.2514/1.G000848

[21] Toda, N., Heiss, J., and Schlee, F., "Spars: The System, Algorithms, and Test Results," *Proceedings of the Symposium on Spacecraft Attitude Determination*, Vol. 1, Aerospace Corp. TR-0066 (6306)-12, El Segundo, CA, 1969, pp. 361–370.

[22] Lefferts, E. J., Markley, F. L., and Shuster, M. D., "Kalman Filtering for Spacecraft Attitude Estimation," *Journal of Guidance, Control, and Dynamics*, Vol. 5, No. 5, 1982, pp. 417–429. https://doi.org/10.2514/3.56190

[23] Markley, F. L., "Attitude Error Representations for Kalman Filtering," *Journal of Guidance, Control, and Dynamics*, Vol. 26, No. 2, 2003, pp. 311–317. https://doi.org/10.2514/2.5048

[24] Axelrad, P., and Ward, L. M., "Spacecraft Attitude Estimation Using the Global Positioning System-Methodology and Results for RADCAL," *Journal of Guidance, Control, and Dynamics*, Vol. 19, No. 6, 1996, pp. 1201–1209. https://doi.org/10.2514/3.21772

[25] Shuster, M., "A Simple Kalman Filter and Smoother for Spacecraft Attitude," *Journal of the Astronautical Sciences*, Vol. 37, No. 1, 1989, pp. 89–106.

[26] Crassidis, J. L., and Markley, F. L., "Unscented Filtering for Spacecraft Attitude Estimation," *Journal of Guidance, Control, and Dynamics*, Vol. 26, No. 4, 2003, pp. 536–542. https://doi.org/10.2514/2.5102

[27] Jia, B., Xin, M., and Cheng, Y., "Sparse Gauss-Hermite Quadrature Filter with Application to Spacecraft Attitude Estimation," *Journal of Guidance, Control, and Dynamics*, Vol. 34, No. 2, 2011, pp. 367–379. https://doi.org/10.2514/1.52016

[28] Kim, S.-G., Crassidis, J. L., Cheng, Y., Fosbury, A. M., and Junkins, J. L., "Kalman Filtering for Relative Spacecraft Attitude and Position Estimation," *Journal of Guidance, Control, and Dynamics*, Vol. 30, No. 1, 2007, pp. 133–143. https://doi.org/10.2514/1.22377

[29] Pittelkau, M. E., "Rotation Vector in Attitude Estimation," *Journal of Guidance, Control, and Dynamics*, Vol. 26, No. 6, 2003, pp. 855–860. https://doi.org/10.2514/2.6929

[30] Trawny, N., and Roumeliotis, S. I., "Indirect Kalman Filter for 3D Attitude Estimation," Dept. of Computer Science and Engineering, Univ. of Minnesota TR 2005-002, Minneapolis, MN, March 2005.

[31] Cheng, Y., and Crassidis, J. L., "Particle Filtering for Attitude Estimation Using a Minimal Local-Error Representation," *Journal of Guidance, Control, and Dynamics*, Vol. 33, No. 4, 2010, pp. 1305–1310. https://doi.org/10.2514/1.47236

[32] Crassidis, J. L., "Sigma-Point Kalman Filtering for Integrated GPS and Inertial Navigation," *IEEE Transactions on Aerospace and Electronic Systems*, Vol. 42, No. 2, 2006, pp. 750–756. https://doi.org/10.1109/TAES.2006.1642588

[33] Hall, J. K., Knoebel, N. B., and McLain, T. W., "Quaternion Attitude Estimation for Miniature Air Vehicles Using a Multiplicative Extended Kalman Filter," *IEEE/ION Position, Location and Navigation Symposium*, IEEE Publ., Piscataway, NJ, 2008, pp. 1230–1237. https://doi.org/10.1109/PLANS.2008.4570043

[34] Reynolds, R. G., "Asymptotically Optimal Attitude Filtering with Guaranteed Convergence," *Journal of Guidance, Control, and Dynamics*, Vol. 31, No. 1, 2008, pp. 114–122. https://doi.org/10.2514/1.30381

[35] Leishman, R. C., and McLain, T. W., "Multiplicative Extended Kalman Filter for Relative Rotorcraft Navigation," *Journal of Aerospace Information Systems*, Vol. 12, No. 12, 2014, pp. 728–744. https://doi.org/10.2514/1.I010236

[36] Gui, H., and Ruiter, A., "Quaternion Invariant Extended Kalman Filtering for Spacecraft Attitude Estimation," *Journal of Guidance, Control, and Dynamics*, Vol. 41, No. 4, 2018, pp. 863–878. https://doi.org/10.2514/1.G003177

[37] Chang, L., Hu, B., and Li, K., "Iterated Multiplicative Extended Kalman Filter for Attitude Estimation Using Vector Observations," *IEEE Transactions on Aerospace and Electronic Systems*, Vol. 52, No. 4, 2016, pp. 2053–2060. https://doi.org/10.1109/TAES.2016.150237

[38] Seba, A., Hadri, A. E., Benziane, L., and Benallegue, A., "Attitude Estimation Using Line-Based Vision and Multiplicative Extended Kalman Filter," *International Conference on Control Automation Robotics Vision*, IEEE Publ., Piscataway, NJ, 2014, pp. 456–461. https://doi.org/10.1109/ICARCV.2014.7064348

[39] Pham, M. D., Low, K. S., Goh, S. T., and Chen, S., "Gain-Scheduled Extended Kalman Filter for Nanosatellite Attitude Determination System," *IEEE Transactions on Aerospace and Electronic Systems*, Vol. 51, No. 2, 2015, pp. 1017–1028. https://doi.org/10.1109/TAES.2014.130204

[40] Santos, D. A., and Gonçalves, P. F., "Attitude Determination of Multirotor Aerial Vehicles Using Camera Vector Measurements," *Journal of Intelligent and Robotic Systems*, Vol. 86, No. 1, 2017, pp. 139–149. https://doi.org/10.1007/s10846-016-0418-0

[41] Yang, Y., Zhou, J., and Loffeld, O., "Quaternion-Based Kalman Filtering on INS/GPS," *15th International Conference on Information Fusion*, IEEE Publ., Piscataway, NJ, 2012, pp. 511–518.

[42] Farsoni, S., Landi, C. T., Ferraguti, F., Secchi, C., and Bonfè, M., "Compensation of Load Dynamics for Admittance Controlled Interactive Industrial Robots Using a Quaternion-Based Kalman Filter," *IEEE Robotics and Automation Letters*, Vol. 2, No. 2, 2017, pp. 672–679. https://doi.org/10.1109/LRA.2017.2651393

[43] Setoodeh, P., Khayatian, A., and Frajah, E., "Attitude Estimation by Separate-Bias Kalman Filter-Based Data Fusion," *Journal of Navigation*, Vol. 57, No. 2, 2004, pp. 261–273. https://doi.org/10.1017/S037346330400270X

[44] Le, H. X., and Matunaga, S., "Real-Time Tuning Separate-Bias Extended Kalman Filter for Attitude Estimation," *Transactions of the Japan Society for Aeronautical and Space Sciences*, Vol. 57, No. 5, 2014, pp. 299–307. https://doi.org/10.2322/tjsass.57.299

[45] Wilthil, E. F., and Brekke, E. F., "Compensation of Navigation Uncertainty for Target Tracking on a Moving Platform," *19th International Conference on Information Fusion*, IEEE Publ., Piscataway, NJ, 2016, pp. 1616–1621.

[46] Vinther, K., Jensen, K. F., Larsen, J. A., and Wisniewski, R., "Inexpensive Cubesat Attitude Estimation Using Quaternions and Unscented Kalman Filtering," *Automatic Control in Aerospace*, Vol. 4, No. 1, 2011, pp. 1–12.

[47] Szczesna, A., and Pruszowski, P., "Model-Based Extended Quaternion Kalman Filter to Inertial Orientation Tracking of Arbitrary Kinematic Chains," *SpringerPlus*, Vol. 5, No. 1, 2016, Paper 1965. https://doi.org/10.1186/s40064-016-3653-8

[48] Hu, J., and Chen, M., "A Sliding-Window Visual-IMU Odometer Based on Tri-Focal Tensor Geometry," *IEEE International Conference on Robotics and Automation*, IEEE Publ., Piscataway, NJ, 2014, pp. 3963–3968. https://doi.org/10.1109/ICRA.2014.6907434

[49] Weiss, S., and Siegwart, R., "Real-Time Metric State Estimation for Modular Vision-Inertial Systems," *2011 IEEE International Conference on Robotics and Automation*, IEEE Publ., Piscataway, NJ, 2011, pp. 4531–4537. https://doi.org/10.1109/ICRA.2011.5979982

[50] Mirzaei, F. M., and Roumeliotis, S. I., "A Kalman Filter-Based Algorithm for IMU-Camera Calibration: Observability Analysis and Performance Evaluation," *IEEE Transactions on Robotics*, Vol. 24, No. 5, 2008, pp. 1143–1156. https://doi.org/10.1109/TRO.2008.2004486

[51] Mourikis, A. I., and Roumeliotis, S. I., "A Multi-State Constraint Kalman Filter for Vision-aided Inertial Navigation," *Proceedings 2007 IEEE International Conference on Robotics and Automation*, IEEE Publ., Piscataway, NJ, 2007, pp. 3565–3572. https://doi.org/10.1109/ROBOT.2007.364024

[52] Koch, D. P., Wheeler, D. O., Beard, R., McLain, T., and Brink, K. M., "Relative Multiplicative Extended Kalman Filter for Observable GPS-Denied Navigation," BYU Ira A. Fulton College of Engineering and Technology Permanent TR-1963, 2017, http://hdl.lib.byu.edu/1877/3919.

[53] Tagliabue, A., Kamel, M., Siegwart, R., and Nieto, J., "Robust Collaborative Object Transportation Using Multiple MAVs," *International Journal of Robotics Research*, Vol. 38, No. 9, 2019, pp. 1020–1044. https://doi.org/10.1177/0278364919854131

[54] Hamer, M., and D'Andrea, R., "Self-Calibrating Ultra-Wideband Network Supporting Multi-Robot Localization," *IEEE Access*, Vol. 6, April 2018, pp. 22,292–22,304. https://doi.org/10.1109/ACCESS.2018.2829020

[55] Greiff, M., Robertsson, A., and Berntorp, K., "Performance Bounds in Positioning with the VIVE Lighthouse System," *IEEE International Conference on Information Fusion*, IEEE Publ., Piscataway, NJ, 2019, https://ieeexplore.ieee.org/abstract/document/9011242.

[56] Beffa, L., Ledergerber, A., and D'Andrea, R., "State Estimate Recovery for Autonomous Quadcopters," *IEEE/RSJ International Conference on Intelligent Robots and Systems*, IEEE Publ., Piscataway, NJ, 2018, pp. 1–7. https://doi.org/10.1109/IROS.2018.8594332

[57] Sola, J., "Quaternion Kinematics for the Error-State KF," Lab. dAnalyse et dArchitecture des Systemes, National Center for Scientific Research, IRI-TR-16-02, Toulouse, France, 2015, https://upcommons.upc.edu/bitstream/handle/2117/104997/1773-Quaternion-kinematics-for-the-error-state-Kalman-filter.pdf.

[58] Chirikjian, G. S., *Stochastic Models, Information Theory, and Lie Groups, Volume 2, : Analytic Methods and Modern Applications*, Vol. 2, Birkhäuser, Basel, Switzerland, 2011. https://doi.org/10.1007/978-0-8176-4944-9

[59] Gallier, J., and Quaintance, J., "Notes on Differential Geometry and Lie Groups," Vol. 4, Univ. of Pennsylvania, Philadelphia, PA, 2012.

[60] Shuster, M. D., "A Survey of Attitude Representations," *Navigation*, Vol. 8, No. 9, 1993, pp. 439–517.

[61] Hall, B. C., "Lie Groups, Lie Algebras, and Representations," *Quantum Theory for Mathematicians*, Springer, New York, 2013, pp. 333–366. https://doi.org/10.1007/978-1-4614-7116-5_16

[62] Gallego, G., and Yezzi, A., "A Compact Formula for the Derivative of a 3-D Rotation in Exponential Coordinates," *Journal of Mathematical Imaging and Vision*, Vol. 51, No. 3, 2015, pp. 378–384. https://doi.org/10.1007/s10851-014-0528-x

[63] Chirikjian, G. S., *Stochastic Models, Information Theory, and Lie Groups, Volume 1, : Classical Results and Geometric Methods*, Applied and Numerical Harmonic Analysis, Birkhäuser, Basel, Switzerland, 2009. https://doi.org/10.1007/978-0-8176-4803-9

[64] Ross, S. M., *Applied Probability Models with Optimization Applications*, Courier Corp., Chelmsford, MA, 2013.

[65] Andrle, M. S., and Crassidis, J. L., "Geometric Integration of Quaternions," *Journal of Guidance, Control, and Dynamics*, Vol. 36, No. 6, 2013, pp. 1762–1767. https://doi.org/10.2514/1.58558

[66] Codling, E., and Hill, N., "Sampling Rate Effects on Measurements of Correlated and Biased Random Walks," *Journal of Theoretical Biology*, Vol. 233, No. 4, 2005, pp. 573–588. https://doi.org/10.1016/j.jtbi.2004.11.008

[67] Ledergerber, A., and D'Andrea, R., "Ultra-Wideband Angle of Arrival Estimation Based on Angle-Dependent Antenna Transfer Function," *Sensors*, Vol. 19, No. 20, 2019, Paper 4466. https://doi.org/10.3390/s19204466

[68] Aggarwal, P., Syed, Z., and El-Sheimy, N., "Hybrid Extended Particle Filter (HEPF) for Integrated Civilian Navigation System," *IEEE/ION Position, Location and Navigation Symposium*, IEEE Publ., Piscataway, NJ, 2008, pp. 984–992. https://doi.org/10.1109/PLANS.2008.4570072

[69] Wang, X., Li, T., Sun, S., and Corchado, J. M., "A Survey of Recent Advances in Particle Filters and Remaining Challenges for Multitarget Tracking," *Sensors*, Vol. 17, No. 12, 2017, p. 2707. https://doi.org/10.3390/s17122707

[70] Doucet, A., De Freitas, N., Murphy, K., and Russell, S., "Rao-Blackwellised Particle Filtering for Dynamic Bayesian Networks," *Proceedings of the Sixteenth Conference on Uncertainty in Artificial Intelligence*, Morgan Kaufmann, San Mateo, CA, 2000, pp. 176–183.

[71] Shariati, H., Moosavi, H., and Danesh, M., "Application of Particle Filter Combined with Extended Kalman Filter in Model Identification of an Autonomous Underwater Vehicle Based on Experimental Data," *Applied Ocean Research*, Vol. 82, Jan. 2019, pp. 32–40. https://doi.org/10.1016/j.apor.2018.10.015

[72] Van Der Merwe, R., Doucet, A., De Freitas, N., and Wan, E., "The Unscented Particle Filter," *Proceedings of the 13th International Conference on Neural Information Processing Systems*, MIT Press, Cambridge, MA, 2000, pp. 563–569.

[73] Simon, D., *Optimal State Estimation: Kalman, H Infinity, and Nonlinear Approaches*, Wiley, New York, 2006.

[74] Bernstein, D. S., *Matrix Mathematics: Theory, Facts, and Formulas with Application to Linear Systems Theory*, Vol. 41, Princeton Univ. Press, Princeton, NJ, 2005.

[75] Galassi, M., Davies, J., Theiler, J., Gough, B., Jungman, G., Alken, P., Booth, M., Rossi, F., and Ulerich, R., *GNU Scientific Library*, Network Theory Ltd., Boston, MA, 2002.

[76] Bourmaud, G., Mégret, R., Giremus, A., and Berthoumieu, Y., "Discrete Extended Kalman Filter on Lie Groups," *21st European Signal Processing Conference*, IEEE Publ., Piscataway, NJ, 2013, pp. 1–5.

[77] Hamer, M., "Scalable Localization and Coordination of Robot Swarms," Ph.D. Thesis, Swiss Federal Inst. of Technology, Zurich, Switzerland, 2019.

[78] Hall, J. K., Knoebel, N. B., and McLain, T. W., "Quaternion Attitude Estimation for Miniature Air Vehicles Using a Multiplicative Extended Kalman Filter," *IEEE/ION Position, Location and Navigation Symposium*, IEEE Publ., Piscataway, NJ, 2008, pp. 1230–1237. https://doi.org/10.1109/PLANS.2008.4570043

[79] Julier, S. J., "The Scaled Unscented Transformation," *Proceedings of the 2002 American Control Conference (IEEE Cat. No. CH37301)*, Vol. 6, IEEE Publ., Piscataway, NJ, 2002, pp. 4555–4559. https://doi.org/10.1109/ACC.2002.1025369

[80] Mäkinen, J., "Rotation Manifold SO(3) and its Tangential Vectors," *Computational Mechanics*, Vol. 42, No. 6, 2008, Paper 907. https://doi.org/10.1007/s00466-008-0293-z

[81] Barfoot, T. D., and Furgale, P. T., "Associating Uncertainty with Three-Dimensional Poses for Use in Estimation Problems," *IEEE Transactions on Robotics*, Vol. 30, No. 3, 2014, pp. 679–693. https://doi.org/10.1109/TRO.2014.2298059

[82] Sommer, H., Gilitschenski, I., Bloesch, M., Weiss, S., Siegwart, R., and Nieto, J., "Why and How to Avoid the Flipped Quaternion Multiplication," *Aerospace*, Vol. 5, No. 3, 2018, Paper 72 https://doi.org/10.3390/aerospace5030072

This article has been cited by:

1. Rajan Gill, Raffaello D'Andrea. 2020. An Annular Wing VTOL UAV: Flight Dynamics and Control. *Drones* **4**:2, 14. [Crossref]